

# BASIC CONCEPTS I AND II

*H. Henke*

Berlin Technical University, Berlin, Germany

## **Abstract**

This is as an introduction to microwave techniques. It does not treat active devices nor special materials used in microwave components, but it deals with the fundamentals of transmission lines, microwave networks, and cavity resonators. It also introduces some basic measurements closely related to this material.

## **1 MICROWAVE ENGINEERING**

The term microwave refers to high-frequency signals with short wavelengths. Because of the short wavelengths standard circuit theory can no longer be used, since the size of components is comparable to the wavelength. Standard circuit theory is a special case of Maxwell's theory, where the components are small in relation to the wavelength. Microwave components are distributed elements, where the fields vary significantly over the physical length of the device. In general, they have to be computed by applying Maxwell's equations and thus the mathematical complexity arises. Microwave engineering tries to reduce the complexity and expresses solutions found by field theory in terms of circuit theory.

The foundations of electromagnetic theory were laid down in Maxwell's theory [1] and proven experimentally by Heinrich Hertz in the years 1887–1891. After a long period of development, the birth of microwave engineering is often attributed to the time of World War II when the Radiation Laboratory was established at MIT, USA, to develop radar theory and technique. Brilliant scientists, including N. Marcuvitz, I.I. Rabi, J.S. Schwinger, H.A. Bethe, E.M. Purcell, C.G. Montgomery, and R.H. Dicke gathered to develop the field of microwaves. Their work is summarized in the 28-volume Radiation Laboratory Series of books [2].

Passive microwave components are transmission lines, filters, couplers, junctions, antennas, ferrite devices and others. Active devices include tubes and solid-state devices, and are used for sources, detectors, amplifiers, mixers, and so on. This paper is an introduction to microwave engineering, treating passive components.

## **2 TRANSMISSION LINES**

Transmission-line theory normally refers to cylindrical (constant cross section) waveguides that support TEM modes or quasi TEM modes, i.e. modes with no (or negligible) longitudinal field components. The field patterns are equal or close to static field distributions and propagate with the velocity of light. These are two-wire lines, coaxial lines, parallel-plate lines, striplines, co-planar striplines and so on. However, much of what we learn in the following can be extended, under certain restrictions, to other waveguides (TM, TE, and hybrid lines) and is therefore of general importance.

### **2.1 Transmission-line equations**

The wave propagation on TEM lines can be calculated, in a formal way, from Maxwell's equations. Here, however, we will use a more intuitive approach and derive it from a short piece of line of length  $dz$ , which is modelled as a lumped-element circuit. As an example we choose a two-wire line.

The current in the wire causes a magnetic field around the axis of the wire and experiences a resistance in transporting the electrons. Therefore, the equivalent circuit has a series inductance  $L'dz$  and a series resistance  $R'dz$  (the prime indicates a quantity per unit length), Fig. 1. Likewise, the voltage

between the conductors includes surface charges on the conductors and a leakage current between the conductors due to dielectric losses. These effects are represented by a shunt capacitance  $C'dz$  and a shunt conductance  $G'dz$ .

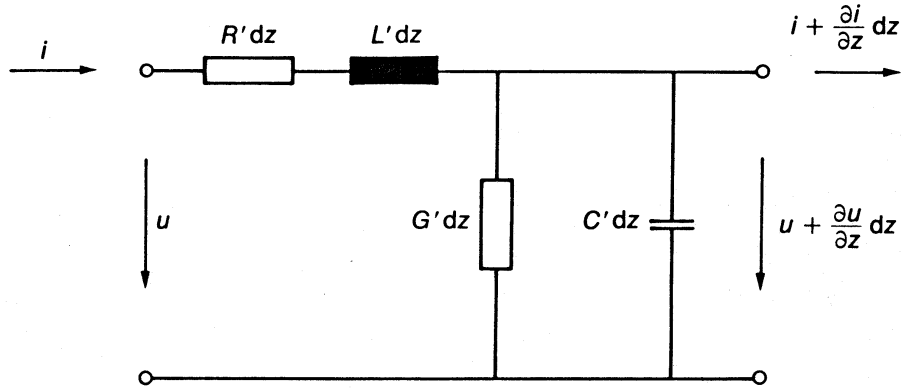


Fig. 1: Equivalent circuit of a piece of line of length  $dz$

Applying Kirchhoff's voltage law

$$u - R' dz i - L' dz \frac{\partial i}{\partial t} - u - \frac{\partial u}{\partial z} dz = 0 \quad (1)$$

and Kirchhoff's current law

$$i - G' dz u - C' dz \frac{\partial u}{\partial t} - i - \frac{\partial i}{\partial z} dz = 0, \quad (2)$$

where we have neglected second-order terms, yields the time-domain form of the transmission-line equations

$$\frac{\partial u}{\partial z} = -R' i - L' \frac{\partial i}{\partial t}, \quad (3)$$

$$\frac{\partial i}{\partial z} = -G' u - C' \frac{\partial u}{\partial t}. \quad (4)$$

The solution of Eqs. (3) and (4) plays an important role in the transmission of steps and impulses. Here, we are interested in the sinusoidal steady-state condition with a time dependence  $\exp(j\omega t)$ , and the equations simplify to

$$\frac{\partial u}{\partial z} = -(R' + j\omega L') i, \quad (5)$$

$$\frac{\partial i}{\partial z} = -(G' + j\omega C') u. \quad (6)$$

To solve Eqs. (5) and (6) we differentiate (5) and substitute (6):

$$\frac{d^2 u}{dz^2} = \gamma^2 u \quad (7)$$

with the complex propagation constant

$$\gamma = \sqrt{(R' + j \omega L')(G' + j \omega C')} = \alpha + j \beta. \quad (8)$$

The solution of Eq. (7) are travelling waves

$$u = u_0^+ e^{j\omega t - \gamma z} + u_0^- e^{j\omega t + \gamma z} \quad (9)$$

and

$$i = \frac{u_0^+}{Z_0} e^{j\omega t + \gamma z} - \frac{u_0^-}{Z_0} e^{j\omega t + \gamma z}, \quad (10)$$

where we used Eq. (5) to find  $i$ , and  $Z_0$  is the **characteristic impedance**

$$Z_0 = \sqrt{\frac{R' + j \omega L'}{G' + j \omega C'}}. \quad (11)$$

The term  $Z_0$  describes the ratio of the voltage and current amplitudes, either for the forward- or backward-travelling wave.

The complex propagation constant (8) consists of the real part

$$\alpha = \sqrt{\frac{1}{2} (R' G' - \omega^2 L' C')} + \frac{1}{2} \sqrt{(R'^2 + \omega^2 L'^2)(G'^2 + \omega^2 C'^2)}, \quad (12)$$

which is the **attenuation constant**, and the imaginary part

$$\beta = \sqrt{-\frac{1}{2} (R' G' - \omega^2 L' C')} + \frac{1}{2} \sqrt{(R'^2 + \omega^2 L'^2)(G'^2 + \omega^2 C'^2)}, \quad (13)$$

which is the **phase constant**. As an example, the forward-travelling wave is shown in Fig. 2. It decays with  $\alpha$  along  $z$  and has a wavelength

$$\lambda = 2\pi/\beta. \quad (14)$$

The phase of each travelling wave is

$$\Phi = \omega t \mp \beta z, \quad (15)$$

which after differentiation with respect to  $t$  determines the phase velocity:

$$v_{ph} = \frac{dz}{dt} = \pm \frac{\omega}{\beta}. \quad (16)$$

## 2.2 Terminated lines

If one excites a wave at the input end of a semi-infinite line there will be only one wave travelling away from the input. The second wave will not be excited (if it were, an infinitely strong source would have to be present at the infinitely remote end of the line). The pattern of the wave is given in Fig. 2.

To treat lines of finite length  $l$  we express  $u$ ,  $i$  in Eqs. (9) and (10) for instance, by their terminal values (here and in the following we drop the time dependence)

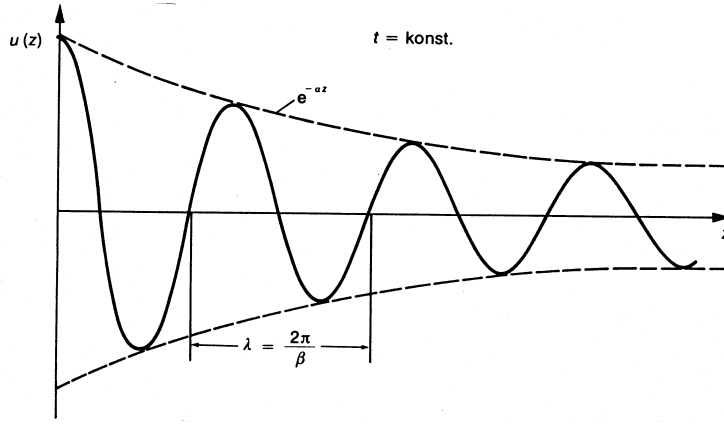


Fig. 2: Voltage of the forward-travelling wave along the line at a fixed time instant

$$u(l) = u_e = u_0^+ e^{-\gamma l} + u_0^- e^{\gamma l}, \quad (17)$$

$$Z_0 i(l) = Z_0 i_e = u_0^+ e^{-\gamma l} - u_0^- e^{\gamma l}, \quad (18)$$

yielding

$$u = \frac{1}{2} (u_e + Z_0 i_e) e^{\gamma(l-z)} + \frac{1}{2} (u_e - Z_0 i_e) e^{-\gamma(l-z)}, \quad (19)$$

$$Z_0 i = \frac{1}{2} (u_e + Z_0 i_e) e^{\gamma(l-z)} - \frac{1}{2} (u_e - Z_0 i_e) e^{-\gamma(l-z)}. \quad (20)$$

First, let us consider a matched line where the terminating impedance  $Z_e$  equals the line impedance  $Z_0$ . Then,

$$Z_e = \frac{u_e}{i_e} Z_0 \quad (21)$$

and the backward-travelling wave vanishes. Similar to the infinitely long line, there is only one forward-travelling wave. At position  $z = l$ , this wave is completely absorbed by the load impedance. The line is **matched**. This is an important situation because an unwanted reflection of the wave is suppressed. Furthermore, since  $Z_0$  is essentially real the matched situation provides an optimal transfer of power to the load.

In the general case of an arbitrary load impedance a part of the forward-travelling wave will be reflected (Fig. 3).

At the end of the line  $u$  and  $i$  are connected by  $u_e = Z_e i_e$  and we obtain for Eq. (19)

$$u = \frac{1}{2} u_e (1 + Z_0/Z_e) e^{\gamma(l-z)} + \frac{1}{2} u_e (1 - Z_0/Z_e) e^{-\gamma(l-z)}, \quad (22)$$

i.e. the ratio of the backward to forward voltage wave at the end of the line is

$$r_e = \frac{Z_e - Z_0}{Z_e + Z_0}. \quad (23)$$

This ratio is called the **reflection coefficient**. If the line is terminated by its impedance, ( $Z_e = Z_0$ ), then  $r = 0$ ; if it is short circuited ( $Z_e = 0$ ),  $r = -1$ ; and in the case of an open circuit ( $Z_e = \infty$ ),  $r = +1$ .

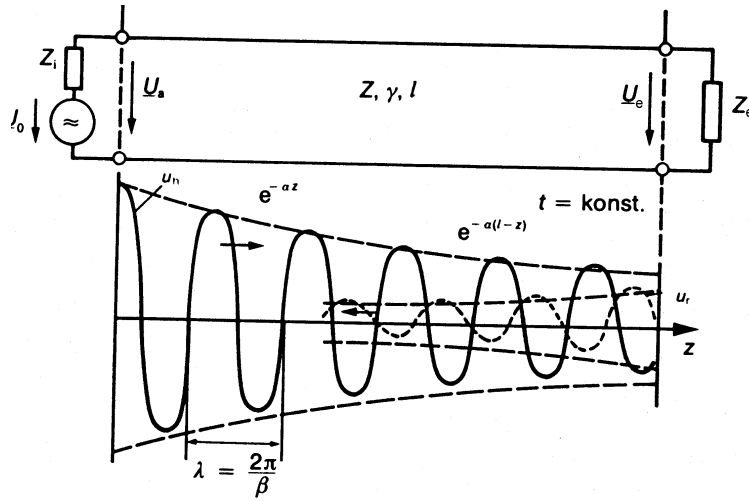


Fig. 3: Line excited by an a.c. voltage and terminated with an arbitrary load

In the last two cases the wave is fully reflected with a cancellation of the voltage or the current for short and open circuits, respectively.

In the case of an arbitrary termination, with the reflection coefficient Eq. (23), the voltage along the line is made up by the two waves Eq. (22). They can be described by complex phasors:

$$u^+(z) = u^+(l) e^{\alpha(l-z)} e^{j\beta(l-z)}, \quad u^+(l) = \frac{1}{2} u_e (1 + Z_0/Z_e), \quad (24)$$

$$u^-(z) = u^-(l) e^{-\alpha(l-z)} e^{-j\beta(l-z)}, \quad u^-(l) = r u^+(l). \quad (25)$$

Going from the line end to the beginning, the phasor of the forward wave increases and rotates counter-clockwise, while the phasor of the backward wave decreases and rotates clockwise. The projection onto the real axis of the vector sum of both phasors is the real voltage.

### 2.3 Terminated lossless line

Typical transmission lines have small losses and for short lengths one can assume  $\alpha l \ll 1$ , then  $\gamma \approx j\beta$  and the voltage and current waves can be written as

$$u(z) = u^+(l) \left[ e^{j\beta(l-z)} + r e^{-j\beta(l-z)} \right], \quad u^+(l) = \frac{u_e}{2} (1 + Z_0/Z_e), \quad (26)$$

$$Z_0 i(z) = u^+(l) \left[ e^{j\beta(l-z)} - r e^{-j\beta(l-z)} \right]. \quad (27)$$

With the distance  $\zeta$  from the line end,  $z = l - \zeta$ , and  $r = |r| \exp(j\vartheta)$ , the voltage magnitude is

$$|u(z)| = |u^+(l)| \left| 1 + |r| e^{j(\vartheta - 2\beta\zeta)} \right|, \quad (28)$$

i.e. it oscillates between maximum values

$$|u|_{\max} = |u^+(l)| |1 + |r|| \quad (29)$$

at positions

$$\zeta_{\max} = (\vartheta - n 2 \pi) / 2 \beta, \quad n = 0, 1, 2, \dots \quad (30)$$

and minimum values

$$|u|_{\min} = |u^+(l)| |1 - |r|| \quad (31)$$

at positions

$$\zeta_{\min} = (\vartheta - (2n + 1) \pi) / 2 \beta. \quad (32)$$

As  $|r|$  increases, the ratio of  $|u|_{\max}$  to  $|u|_{\min}$  increases, so a measure of the mismatch of the line is the **standing wave ratio**, defined as

$$SWR = \frac{|u|_{\max}}{|u|_{\min}} = \frac{1 + |r|}{1 - |r|}. \quad (33)$$

The *SWR* is a real number between 1 and  $\infty$ , where 1 implies a matched line and  $\infty$  refers to an open or shortened line. From Eqs. (29) to (32) it follows that the distance between subsequent maxima or minima is  $\pi/\beta = \lambda/2$ , while the distance between a maximum and a minimum is  $\pi/2\beta = \lambda/4$ .

While the voltage amplitude is oscillatory with position on the line, the time-average power flow is constant. From Eqs. (26) and (27) follow

$$\begin{aligned} P_{av} &= \frac{1}{2} \operatorname{Re} \{u(z) i^*(z)\} = \frac{1}{2Z_0} |u^+(l)|^2 \operatorname{Re} \left\{ 1 - r^* e^{j2\beta(l-z)} + r e^{-j2\beta(l-z)} - |r|^2 \right\} \\ &= \frac{|u^+(l)|^2}{2Z_0} \operatorname{Re} \left\{ 1 - |r|^2 + 2j \operatorname{Im} \left( r e^{-j2\beta(l-z)} \right) \right\} \\ &= \frac{1}{2Z_0} |u^+(l)|^2 (1 - |r|^2), \end{aligned} \quad (34)$$

which shows that the average power flow is constant along the line and that the power delivered to the load impedance is equal to the incident power  $|u^+(l)|^2/2Z_0$  minus the reflected power  $|ru^+(l)|^2/2Z_0$ .

As shown above, the voltage is oscillating on the line and the real power flow is constant. It can therefore be concluded that the impedance seen looking into the line must vary with position. At a distance  $\zeta = 1 - z$  from the load the **input impedance** follows from Eqs. (26) and (27) and Eq. (23) as

$$\begin{aligned} Z_{in} &= \frac{u(\zeta)}{i(\zeta)} \\ &= Z_0 \frac{\exp(j\beta\zeta) + r \exp(-j\beta\zeta)}{\exp(j\beta\zeta) - r \exp(-j\beta\zeta)} \\ &= Z_0 \frac{Z_e \cos \beta\zeta + j Z_0 \sin \beta\zeta}{j Z_e \sin \beta\zeta + Z_0 \cos \beta\zeta} \\ &= Z_0 \frac{Z_e + j Z_0 \tan \beta\zeta}{Z_e + Z_0 \tan \beta\zeta}. \end{aligned} \quad (35)$$

This important result gives the input impedance of a length  $\zeta$  of a transmission line with an arbitrary terminating impedance.

## 2.4 Impedance transformation

On a lossy line the voltage and current waves follow Eqs. (26) and (27) with  $j\beta$  replaced by  $\gamma$ . Then, the input impedance corresponding to Eq. (35) is

$$Z_{in} = Z_0 \frac{Z_e + Z_0 \tanh \gamma \zeta}{Z_0 + Z_e \tanh \gamma \zeta}. \quad (36)$$

We write

$$\tanh \gamma \zeta = \frac{\tanh \alpha \zeta + j \tan \beta \zeta}{1 + j \tanh \alpha \zeta \cdot \tan \beta \zeta}. \quad (37)$$

$$Z_e/Z_0 = \tanh(x + j y), \quad (38)$$

and obtain for Eq. (36)

$$\frac{Z_{in}}{Z_0} = \tanh [x + \alpha \zeta + j (y + \beta \zeta)]. \quad (39)$$

Six special cases are of interest:

1. The **long lossy line**, where  $\alpha \zeta \gg 1$ , then

$$\tanh \alpha \zeta \approx 1, \quad \tanh \gamma \zeta \approx 1 \quad (40)$$

and

$$Z_{in} \approx Z_0. \quad (41)$$

The input impedance is independent of the terminating impedance and equals the line impedance.

2. A **small mismatch** with  $Z_e = Z_0(1 + x)$ ,  $|x| \ll 1$ , then

$$\frac{Z_{in}}{Z_0} = \frac{1 + x/(1 + \tanh \gamma \zeta)}{1 + x \tanh \gamma \zeta/(1 + \tanh \gamma \zeta)} \approx 1 + x \frac{1 - \tanh \gamma \zeta}{1 + \tanh \gamma \zeta} = 1 + x e^{-2\gamma \zeta}, \quad (42)$$

i.e. the smaller the mismatch  $x$  and the larger the attenuation  $\alpha \zeta$ , is the better the input impedance approximates the line impedance. The deviation depends on  $\beta \zeta$ , but is always smaller than  $|x| \exp(-2\alpha \zeta)$ . This is a good estimate for how strong a small mismatch appears at the input.

3. Line terminated in a short circuit,  $Z_e = 0$ , then

$$Z_{in}^s = Z_0 \tanh \gamma \zeta \quad (43)$$

4. Line terminated in an open circuit,  $Z_e = \infty$ , then

$$Z_{in}^s = Z_0 \coth \gamma \zeta. \quad (44)$$

From Eqs. (43) and (44) follows

$$Z_0 = \sqrt{Z_{in}^0 Z_{in}^s} \quad (45)$$

$$\tanh \gamma \zeta = \sqrt{Z_{in}^s/Z_{in}^0} \quad (46)$$

or

$$e^{2\gamma\zeta} = \left(1 + \sqrt{Z_{in}^s/Z_{in}^0}\right) / \left(1 - \sqrt{Z_{in}^s/Z_{in}^0}\right), \quad (47)$$

and line impedance as well as propagation constant can be determined from measuring the input impedance of the open and shorted line.

Particularly useful for impedance transformation are lossless lines (or short lines with small losses). They transform impedances with no losses.

#### 5. The $\lambda/4$ -impedance inverter

A line of length  $\zeta = \lambda/4$  has  $\beta\zeta = \pi/2$  and the input impedance (35) is

$$Z_{in} = Z_0^2/Z_e. \quad (48)$$

A real load  $Z_e = R_e$  can be transformed into any real impedance  $Z_{in} = R_{in}$  by choosing  $Z_0 = \sqrt{R_e R_{in}}$ . However, since  $\beta$  depends on  $\omega$ , the exact transformation is obtained only at the right frequency. For a broad band transformation several cascaded  $\lambda/4$  inverters with different  $Z_0$  are used.

#### 6. The $\lambda/2$ transformer

If the line has a length  $\zeta = \lambda/2$ , then  $\beta\zeta = \pi$  and the input impedance (48) equals the termination

$$Z_{in} = Z_e. \quad (49)$$

## 2.5 The Smith chart

The Smith chart was developed by P. Smith at the Bell Telephone Laboratories in 1939. It is a graphical aid to solve transmission line problems.

We express the complex ratio of terminating impedance to line impedance by

$$\frac{Z_e}{Z_0} = z = x + j y \quad (50)$$

and write the reflection coefficient (23) as a function of  $z$ :

$$r = r_r + j r_j = \frac{z - 1}{z + 1}. \quad (51)$$

Then, the Smith chart maps the complex  $z$ -plane into the polar plot of the voltage reflection coefficient, Fig. 4(a). We invert Eq. (51),

$$z = \frac{1 + r}{1 - r},$$

and split it into real and imaginary parts:

$$x = \frac{1 - r_r^2 - r_i^2}{(1 - r_r)^2 + r_i^2}, \quad y = \frac{2 r_i}{(1 - r_r)^2 + r_i^2}.$$

The last two equations can be rearranged such that they represent two sets of circles in the  $r$ -plane:

$$\left(r_r - \frac{x}{1+x}\right)^2 + r_i^2 = \frac{1}{(1+x)^2}, \quad (52)$$

$$(r_r - 1)^2 + \left(r_i - \frac{1}{y}\right)^2 = \frac{1}{y^2}. \quad (53)$$



Equation (52) defines resistance circles for  $x = \text{const.}$  and Eq. (53) defines reactance circles for  $y = \text{const.}$  All resistance circles have centres on the horizontal  $r_i = 0$  axis, and pass through the point  $r = 1$ . The centres of the reactance circles lie on the vertical  $r_r = 1$  line, and the circles pass also through the point  $r = 1$ .

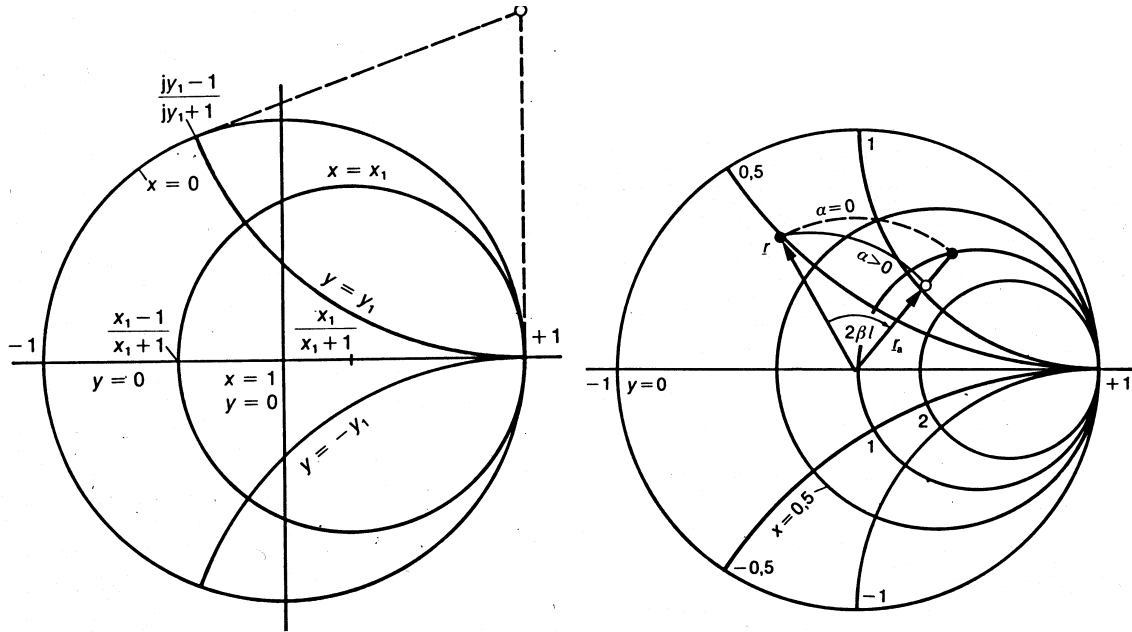


Fig. 4: (a) Construction of a Smith chart; (b) Impedance transformation in the Smith chart

The Smith chart allows impedance transformations in a convenient way. Following the arguments in Section 2.2 and defining the reflection coefficient at any position  $z = 1 - \zeta$  as the ratio of backward to forward voltage wave, we obtain from Eqs. (22) and (23)

$$r(\zeta) = \frac{Z_e - Z_0}{Z_e + Z_0} e^{-2\gamma\zeta} = r_e^{-2\alpha\zeta} e^{-j2\beta\zeta}. \quad (54)$$

Then, we find for the impedance at position  $\zeta$

$$Z_{in}(\zeta) = \frac{u(\zeta)}{i(\zeta)} = Z_0 \frac{1 + r(\zeta)}{1 - r(\zeta)} \quad (55)$$

or after inversion

$$r(\zeta) = \frac{Z_{in}(\zeta)/Z_0 - 1}{Z_{in}(\zeta)/Z_0 + 1}. \quad (56)$$

The relations (55) and (56), together with the Smith chart (Fig. 4(b)), now allow the input impedance to be determined when the terminating impedance  $z$  is given. We find  $z$  in the chart and read the corresponding reflection coefficient  $r(0)$ . Corresponding to Eq. (55) we rotate  $r$  by  $-2\beta\zeta$  and demagnify it by  $\exp(-2\alpha\zeta)$ . The readings of the new point determine  $Z_{in}(\zeta)/Z_0$ .

### 3 MICROWAVE NETWORKS

Microwave networks consist of different elements connected by lines. An element may have several 'ports' (connections with lines), Fig. 5. At each port we use the voltages and currents we have defined previously. The relations between the port quantities define the element.

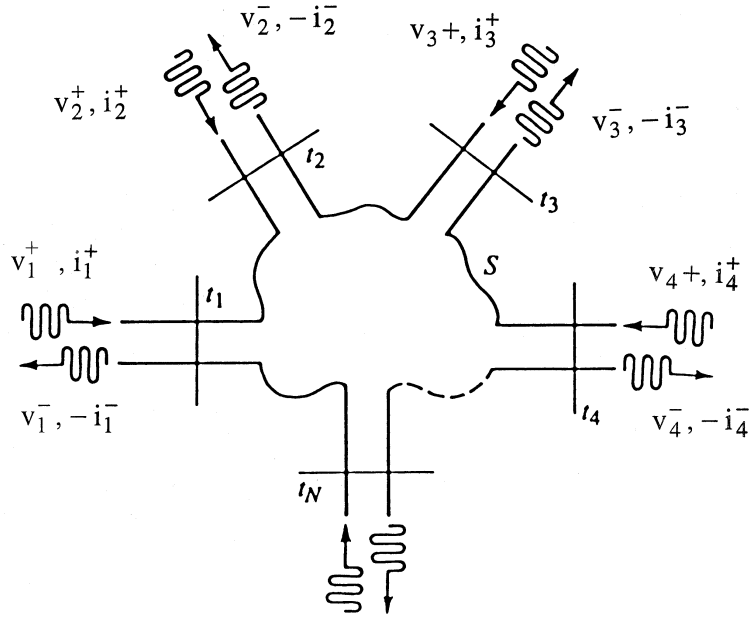


Fig. 5: An  $N$ -port microwave network

### 3.1 Impedance and admittance matrices

Let us consider an  $N$ -port network as shown in Fig. 5. At the  $n$ th port, in a well-defined terminal plane  $t_n$ , the voltage and current are given by

$$u_n = u_n^+ + u_n^-, \quad i_n = i_n^+ - i_n^-. \quad (57)$$

The terminal plane  $t_n$  is important in providing a phase reference for the voltage and current phasors. Then, assuming linear networks, the relation between the voltages and currents at the different parts can be expressed by the **impedance matrix**

$$\mathbf{U} = \mathbf{Z} \mathbf{I}, \quad \mathbf{Z} = \begin{bmatrix} Z_{11} & Z_{12} & \dots & Z_{1N} \\ Z_{21} & Z_{22} & \dots & \vdots \\ \vdots & \vdots & \dots & \vdots \\ Z_{N1} & Z_{N2} & \dots & Z_{NN} \end{bmatrix}, \quad \mathbf{U} = \begin{bmatrix} u_1 \\ u_2 \\ \vdots \\ u_N \end{bmatrix}, \quad \mathbf{I} = \begin{bmatrix} i_1 \\ i_2 \\ \vdots \\ i_N \end{bmatrix}, \quad (58)$$

or **admittance bmatrix**

$$\mathbf{I} = \mathbf{Y} \mathbf{U}, \quad \mathbf{Y} = \mathbf{Z}^{-1}. \quad (59)$$

The elements of, for instance, the impedance matrix can be found as

$$Z_{ij} = \frac{u_i}{i_j}, \quad \text{if } i_k = 0 \text{ for } k \neq j, \quad (60)$$

that is by driving port  $j$  with  $i_j$ , while all other ports are open, and measuring the open-circuit voltage at port  $i$ . Thus,  $Z_{ii}$  is the input impedance of port  $i$  when all other ports are open-circuited, and  $Z_{ij}$  is the transfer impedance between ports  $i$  and  $j$  when all other ports are open-circuited.

In general, each  $Z_{ij}$  and  $Y_{ij}$  may be complex, and an  $N$ -port network will have  $2N^2$  independent quantities. In practice, however, many networks are reciprocal or lossless, or both. If the network is

reciprocal the impedance and admittance matrices are symmetric. If the network is lossless, the elements  $Z_{ii}$ ,  $Y_{ii}$  are purely imaginary.

A network is **reciprocal** if it does not contain active devices or non-reciprocal material such as ferrites or plasmas. Reciprocity is a consequence of Maxwell's equations (Lorentz reciprocity theorem) and can be shown easily [3]. Here, we will only state the consequences. Let us shorten all ports but the first and second. Then, a current  $i_1'$  applied to port 1 will create a voltage  $u_2'$  at port 2. Conversely, a current  $i_2''$  at port 2 will create a voltage  $u_1''$  at port 1. Reciprocity means that the transfer impedances are equal,

$$\frac{u_2'}{i_1'} = \frac{u_1''}{i_2''}, \quad \text{or} \quad Z_{21} = Z_{12},$$

and since this is valid for any two ports the impedance matrix  $\mathbf{Z}$  is symmetric. Its inverse, the admittance matrix  $\mathbf{Y}$  is also symmetric.

In **lossless networks** the averaged real power delivered to the network must be zero. We start with all ports but the  $i$ th open and obtain

$$P_{av} = \frac{1}{2} \operatorname{Re}\{u_i i_i^*\} = \frac{1}{2} \operatorname{Re}\{Z_{ii}\} |i_1|^2 = 0$$

or  $\operatorname{Re}\{Z_{ii}\} = 0$ . Next, we drive the  $i$ th and  $j$ th port with  $i_i$  and  $i_j$ ,

$$\begin{aligned} P_{av} &= \frac{1}{2} \operatorname{Re}\{u_i i_i^* + u_j i_j^*\} = \frac{1}{2} \operatorname{Re}\{Z_{ii} |i_i|^2 + Z_{jj} |i_j|^2 + Z_{ij} i_j i_i^* + Z_{ji} i_i i_j^*\} \\ &= \frac{1}{2} \operatorname{Re}\{Z_{ij} i_j i_i^* + Z_{ji} i_i i_j^*\} = \frac{1}{2} \operatorname{Re}\{Z_{ij} (i_i i_j^* + i_i^* i_j)\} = 0, \end{aligned}$$

and since  $i_i i_j^* + i_i^* i_j$  is real it follows that  $\operatorname{Re}\{Z_{ij} = 0\}$ . Here, we have used  $Z_{ij} = Z_{ji}$ . That means the elements of the impedance and admittance matrix are purely imaginary for lossless and reciprocal networks.

Often, in practice, the network is a symmetric 2-port network and the impedance matrix reduces to

$$\mathbf{Z} = \begin{bmatrix} Z_{11} & Z_{12} \\ Z_{21} & Z_{22} \end{bmatrix}. \quad (61)$$

One possible equivalent network is the T-junction shown in Fig. 6(a). The elements are easily found by applying open circuits:

$$\begin{aligned} Z_{11} &= \left. \frac{u_1}{i_1} \right|_{i_2=0} = Z_a + Z_c, \\ Z_{22} &= \left. \frac{u_2}{i_2} \right|_{i_1=0} = Z_b + Z_c, \\ Z_{12} &= \left. \frac{u_1}{i_2} \right|_{i_1=0} = Z_c. \end{aligned} \quad (62)$$

The equivalent network for the admittance matrix is normally a  $\pi$  network, Fig. 6(b). The elements can be found by short circuits:

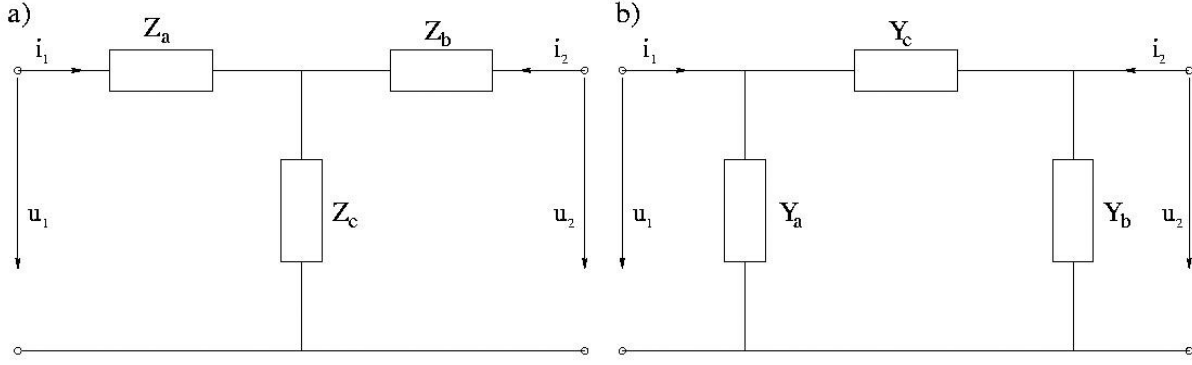


Fig. 6: (a) Equivalent T network with a symmetric impedance matrix; (b) Equivalent  $\pi$  network for a symmetric admittance matrix

$$\begin{aligned}
 Y_{11} &= \left. \frac{i_1}{u_1} \right|_{u_2=0} = Y_a + Y_c, \\
 Y_{22} &= \left. \frac{i_2}{u_2} \right|_{u_1=0} = Y_b + Y_c, \\
 Y_{12} &= \left. \frac{i_1}{u_2} \right|_{u_1=0} = -Y_c.
 \end{aligned} \tag{63}$$

### 3.2 Scattering matrix

The description of microwave networks by voltages and currents is not always the best choice. This has to do with problems of measuring voltages and currents at high frequencies but also with difficulties in defining voltages and currents for non-TEM lines (waveguides). Therefore, the description of networks by impedance and admittance matrices becomes somewhat an abstraction. A representation more in accordance with direct measurements is given by the scattering matrix  $\mathbf{S}$ . The scattering matrix also provides a complete description of the network as seen at its  $N$  ports. It relates the incoming waves to the reflected waves.

Consider the  $N$ -port of Fig. 5, where  $u_n^+$  and  $u_n^-$  are the amplitudes of the incoming and reflected waves, respectively. Referring to Eqs. (9) and (10) and choosing the port plane  $t_n$  as a reference plane we can normalize the amplitudes of the voltage and current waves,

$$a_n = u_n^+ / \sqrt{Z_0}, \quad b_n = u_n^- / \sqrt{Z_0}, \tag{64}$$

such that the averaged real power delivered into port  $n$  is

$$\begin{aligned}
 P_{av} &= \frac{1}{2} \operatorname{Re}\{u_n i_n^*\} = \frac{1}{2} \operatorname{Re}\{\sqrt{Z_0} (a_n + b_n) \frac{1}{Z_0} (a_n^* - b_n^*)\} \\
 &= \frac{1}{2} \operatorname{Re}\{|a_n|^2 - |b_n|^2 + b_n a_n^* - a_n b_n^*\} = \frac{1}{2} (|a_n|^2 - |b_n|^2),
 \end{aligned} \tag{65}$$

i.e. the incoming power is given by  $|a_n|^2/2$  and the reflected power by  $|b_n|^2/2$ .

The relation between the wave amplitudes  $a_i, b_i$  is given by a system of  $N$  linear equations

$$\mathbf{b} = \mathbf{S} \mathbf{a}, \quad \mathbf{S} = \begin{bmatrix} S_{11} & S_{12} & \dots & S_{1N} \\ S_{21} & S_{22} & \dots & S_{2N} \\ \vdots & \vdots & \ddots & \vdots \\ S_{N1} & S_{N2} & \dots & S_{NN} \end{bmatrix}, \quad \mathbf{a} = \begin{bmatrix} a_1 \\ a_2 \\ \vdots \\ a_N \end{bmatrix}, \quad \mathbf{b} = \begin{bmatrix} b_1 \\ b_2 \\ \vdots \\ b_N \end{bmatrix}, \quad (66)$$

and the system matrix is the **scattering matrix**. The elements are found by

$$S_{ij} = \frac{b_i}{a_j}, \quad \text{if } a_k = 0 \text{ for } k \neq j. \quad (67)$$

That is,  $S_{ii}$  is the reflection coefficient at port  $i$  when all other ports are matched, and  $S_{ij}$  is the transmission coefficient for a wave coming in at port  $j$  and going out at port  $i$  when all ports are matched.

For networks satisfying reciprocity, the scattering matrix is symmetric, as are the impedance and admittance matrices.

If the network is loss-free, then the real power coming out of the ports must equal the real power delivered to the ports

$$\frac{1}{2} \mathbf{b}^t \mathbf{b}^* = \frac{1}{2} \mathbf{a}^t \mathbf{a}^*,$$

which we write as

$$(\mathbf{S} \mathbf{a})^t (\mathbf{S} \mathbf{a})^* = \mathbf{a}^t \mathbf{S}^t \mathbf{S}^* \mathbf{a}^* = \mathbf{a}^t \mathbf{a}^* = \mathbf{a}^t \mathbf{1} \mathbf{a}^*.$$

Thus

$$\mathbf{S}^t \mathbf{S}^* = \mathbf{1},$$

and the transpose is the conjugate of the inverse matrix

$$\mathbf{S}^t = (\mathbf{S}^{-1})^*, \quad (68)$$

which is called a **unitary matrix**. We can write these relations as sums,

$$\sum_{k=1}^N S_{ki} S_{ki}^* = 1, \quad (69)$$

$$\sum_{k=1}^N S_{ki} S_{kj}^* = 0, \quad i \neq j, \quad i, j = 1, 2, \dots, N, \quad (70)$$

stating that the columns of the scattering matrix are orthonormal.

Equations (69) and (70) reduce the number of independent quantities but they also impose restrictions on what can or cannot be done with loss-free junctions. Consider for instance the loss-free power divider or power combiner of Fig. 7. If sources are introduced at ports 1 and 2 with the combined power obtained at 3, one might wish to have  $S_{12} = S_{21} = 0$  in order to eliminate direct interaction between the sources. But Eq. (70) with  $i = 1, j = 2$  gives

$$S_{11} S_{12}^* + S_{21} S_{22}^* + S_{31} S_{32}^* = 0,$$

requiring either  $S_{31}$  or  $S_{32}$  to be equal to zero and thus eliminating one of the two desired couplings. The junction will act as a power combiner, but the sources will interact, and if they are not identical in magnitude and phase, one source will feed power to the other.

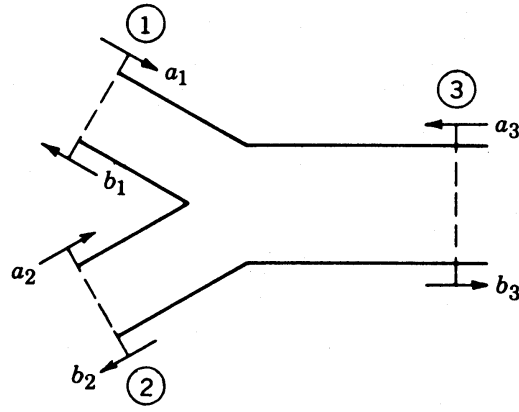


Fig. 7: A Y-junction power combiner

In dealing with cascaded circuits, the scattering formalism is not convenient. For that purpose we restrict ourselves to 2-port circuits and rearrange the scattering matrix such that the amplitudes  $a_2, b_2$  are the independent and  $b_1, a_1$  the dependent variables:

$$\begin{bmatrix} b_1 \\ a_1 \end{bmatrix} = \begin{bmatrix} T_{11} & T_{12} \\ T_{21} & T_{22} \end{bmatrix} \begin{bmatrix} a_2 \\ b_2 \end{bmatrix}; \quad (71)$$

with

$$T_{11} = S_{12} - S_{11} S_{22}/S_{21}, \quad T_{12} = S_{11}/S_{21}, \quad T_{21} = -S_{22}/S_{21}, \quad T_{22} = 1/S_{21}.$$

Now, the output wave  $b_2$  of a first circuit is the input wave  $a'_1$  of a subsequent circuit, and the input  $a_2$  is the output  $b'_1$ , see Fig. 8. Simple multiplication of the transfer matrices gives the overall matrix

$$\begin{bmatrix} b_1 \\ a_1 \end{bmatrix} = T \begin{bmatrix} a_2 \\ b_2 \end{bmatrix}, \quad \begin{bmatrix} b'_1 \\ a'_1 \end{bmatrix} = T' \begin{bmatrix} a'_2 \\ b'_2 \end{bmatrix};$$

and since

$$\begin{bmatrix} a_2 \\ b_2 \end{bmatrix} = \begin{bmatrix} b'_1 \\ a'_1 \end{bmatrix},$$

$$\begin{bmatrix} b_1 \\ a_1 \end{bmatrix} = T T' \begin{bmatrix} a'_2 \\ b'_2 \end{bmatrix}. \quad (72)$$

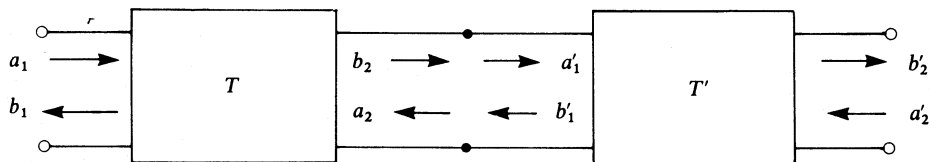


Fig. 8: Cascade connection of two 2-port networks

### 3.3 Some common microwave elements

T-junction power dividers, Fig. 9, are simple 3-port networks that can be used for power division or combining. As mentioned above, such a network cannot be lossless, reciprocal and matched at all ports. If it is lossless and reciprocal the scattering matrix must be symmetric and Eqs. (69) and (70) hold. In case of the H-plane T, for instance, we can further assume that the waves going out from the ports 1 and 2 are symmetric if port 3 is driven, i.e.  $S_{13} = S_{23}$ , and that port 3 is matched,  $S_{33} = 0$ . Then Eqs. (69) and (70) reduce to

$$\begin{aligned} |S_{11}|^2 + |S_{12}|^2 + |S_{13}|^2 &= 1, \\ |S_{12}|^2 + |S_{22}|^2 + |S_{13}|^2 &= 1, \\ 2|S_{13}|^2 &= 1, \\ S_{11} S_{12}^* + S_{12} S_{22}^* + |S_{13}|^2 &= 0, \\ S_{11} S_{13}^* + S_{12} S_{13}^* &= 0, \\ S_{12} S_{13}^* + S_{22} S_{13}^* &= 0, \end{aligned}$$

which gives

$$S_{11} = S_{22} = -S_{12}, \quad |S_{13}| = 1/\sqrt{2}, \quad |S_{11}| = 1/2$$

and, after choosing the reference planes such that the elements are real,

$$\mathbf{S}_H = \frac{1}{2} \begin{bmatrix} 1 & -1 & \sqrt{2} \\ -1 & 1 & \sqrt{2} \\ \sqrt{2} & \sqrt{2} & 0 \end{bmatrix}. \quad (73)$$

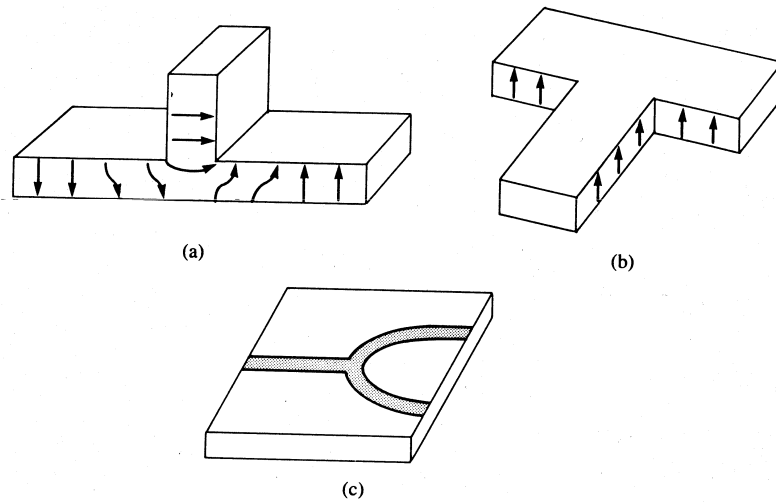


Fig. 9: Various T-junction dividers: (a) E-plane waveguide; (b) H-plane waveguide; (c) Microstrip

If the 3-port network is non-reciprocal,  $S_{ij} \neq S_{ji}$ , then the condition of input matching at all ports,  $S_{ii} = 0$ , can be satisfied. We further assume a lossfree device and Eqs. (69) and (70) become

$$\begin{aligned}
|S_{21}|^2 + |S_{31}|^2 &= 1, & S_{31} S_{32}^* &= 0; \\
|S_{12}|^2 + |S_{32}|^2 &= 1, & S_{21} S_{23}^* &= 0; \\
|S_{13}|^2 + |S_{23}|^2 &= 1, & S_{12} S_{13}^* &= 0.
\end{aligned}$$

The equations can be satisfied in one of two ways

$$S_{12} = S_{23} = S_{31} = 0, \quad |S_{21}| = |S_{13}| = |S_{32}| = 1$$

or

$$S_{21} = S_{13} = S_{32} = 0, \quad |S_{31}| = |S_{12}| = |S_{23}| = 1.$$

The result is that  $S_{ij} \neq S_{ji}$  for  $i \neq j$ , i.e. the device is non-reciprocal. The two solutions are shown in Figs. 10(a) and (b). The first solution is a device where the power coming in at port 1 exits at port 2, and power coming in at port 2 will exit at 3 and so on. Such a device is called a circulator and allows the separation of a source at port  $i$  from reflections coming from a load at port  $i+1$ . In the second solution the direction of power flow is changed. Circulators employ generally anisotropic materials, such as ferrites, and can be realized in very different ways. Two solutions are shown in Figs. 10(c) and (d).

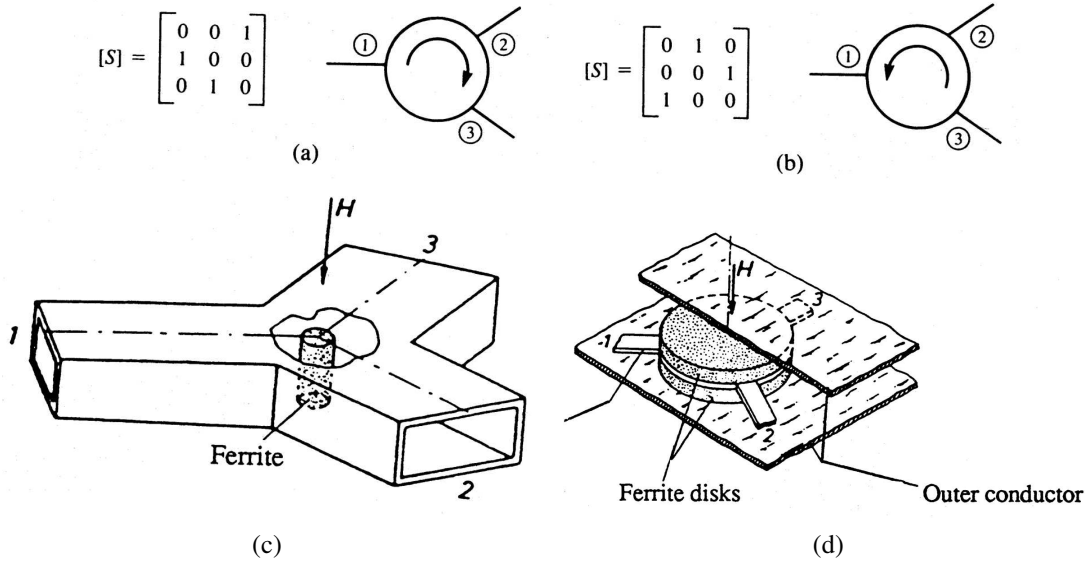


Fig. 10: Different circulators. (a) Clockwise circulation; (b) counter-clockwise circulation; (c) waveguide circulator; (d) stripline circulator.

Two examples of 4-port networks are directional couplers and hybrids, see Fig. 11. We assume a reciprocal loss-free network with all four ports matched,  $S_{ii} = 0$ . We further assume isolation between the ports 1-4 and 2-3,  $S_{14} = S_{23} = 0$ . Then, the scattering matrix reduces to

$$\mathbf{S} = \begin{bmatrix} 0 & S_{12} & S_{13} & 0 \\ S_{12} & 0 & 0 & S_{24} \\ S_{13} & 0 & 0 & S_{34} \\ 0 & S_{24} & S_{34} & 0 \end{bmatrix} \quad (74)$$



with four unknowns. Equations (69) and (70) yield for  $i = j$

$$|S_{12}|^2 + |S_{13}|^2 = 1, |S_{12}|^2 + |S_{24}|^2 = 1, |S_{13}|^2 + |S_{34}|^2 = 1, |S_{24}|^2 + |S_{34}|^2 = 1, \quad (75)$$

implying  $|S_{13}| = |S_{24}|$  and  $|S_{12}| = |S_{34}|$ . Furthermore, we select the terminal plane  $t_2$  with respect to  $t_1$  so that  $S_{12}$  is real and positive, and similarly 4 with respect to 3 so that  $S_{34}$  is real and positive, i.e.

$$S_{12} = S_{34} = \alpha.$$

From Eqs. (69) and (70) with  $i \neq j$  remains

$$\begin{aligned} S_{12} S_{24}^* + S_{13} S_{34}^* &= 0, \\ S_{12} S_{13}^* + S_{24} S_{34}^* &= 0, \end{aligned}$$

requiring  $S_{13} = -S_{24}^*$ .  $S_{13}$  and  $S_{24}$  can only differ in phase, therefore

$$S_{13} = \beta e^{j\varphi}, \quad S_{24} = \beta e^{j\vartheta}$$

and the relation between phases is

$$\varphi + \vartheta = \pi + 2n\pi.$$

Ignoring integer multiples of  $2\pi$ , there are two choices:

- symmetrical coupler,  $\varphi = \vartheta = \pi/2$ ,
- antisymmetrical coupler,  $\varphi = 0, \vartheta = \pi$ .

The related scattering matrices are

$$\mathbf{S}_s = \begin{bmatrix} 0 & \alpha & j\beta & 0 \\ \alpha & 0 & 0 & j\beta \\ j\beta & 0 & 0 & \alpha \\ 0 & j\beta & \alpha & 0 \end{bmatrix}, \quad \mathbf{S}_{as} = \begin{bmatrix} 0 & \alpha & \beta & 0 \\ \alpha & 0 & 0 & -\beta \\ \beta & 0 & 0 & \alpha \\ 0 & -\beta & \alpha & 0 \end{bmatrix}. \quad (76)$$

Note that the two couplers differ only in the choice of reference planes. Also, the constants  $\alpha, \beta$  are not independent because of Eq. (75),

$$\alpha^2 + \beta^2 = 1;$$

therefore, an ideal directional coupler has only one degree of freedom. The coupling mechanism is either hole coupling, Fig. 11, where the strength is adjusted by the number and the size of the holes, or coupled transmission lines, where the distance between lines determines the strength.

Hybrid couplers are special cases of directional couplers, where the coupling factor is 3 dB, i.e.  $\alpha = \beta = 1/\sqrt{2}$ . There are two types of hybrid:

- Quadrature hybrid with  $90^\circ$  phase shift between ports 2 and 3 when fed at port 1. It is a symmetrical coupler, see Fig. 12.
- Magic-T or rat-race hybrid with  $180^\circ$  phase difference between ports 2 and 3 when fed at port 4. It is an antisymmetrical coupler, see Fig. 12.

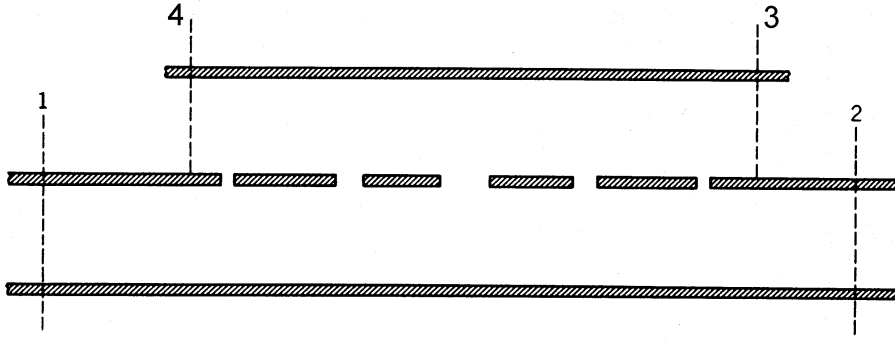


Fig. 11: Hole-coupled directional coupler

Directional couplers are usually characterized by three quantities:

$$\begin{aligned}
 \text{coupling} & \quad C = 10 \log P_1/P_3 = -20 \log \beta \text{ dB}, \\
 \text{directivity} & \quad D = 10 \log P_3/P_4 = 20 \log \frac{\beta}{|S_{14}|} \text{ dB}, \\
 \text{isolation} & \quad I = 10 \log P_1/P_4 = -20 \log |S_{14}| \text{ dB}.
 \end{aligned} \tag{77}$$

$C$  indicates the fraction of the input power which is coupled to the output.  $D$  is a measure of the coupler's ability to isolate forward and backward waves, as is  $I$ . These quantities are related as follows:

$$I = D + C.$$

An ideal coupler [Eq. (76)] has infinite directivity and isolation.

## 4 CAVITY RESONATORS

Cavity resonators have an infinite number of oscillatory modes. Each mode is characterized by its resonant frequency, the stored electromagnetic energy and the losses dissipated in the walls and eventually also radiated into external circuits. Near resonance, a mode can be modelled by an equivalent lumped-element resonant circuit.

### 4.1 Lumped-element resonant circuits

Lumped-element resonant circuits can be series or parallel circuits (Fig. 13).

#### Series circuit

The input impedance is

$$Z_{in} = R + j \omega L + \frac{1}{j \omega C} \tag{78}$$

and the complex power delivered to the circuit is

$$\begin{aligned}
 P_{in} &= \frac{1}{2} u i^* = \frac{1}{2} Z_{in} |i|^2 = \frac{1}{2} |i|^2 \left( R + j \omega L + \frac{1}{j \omega C} \right) \\
 &= P_{loss} + 2 j \omega (W_m - W_e),
 \end{aligned} \tag{79}$$

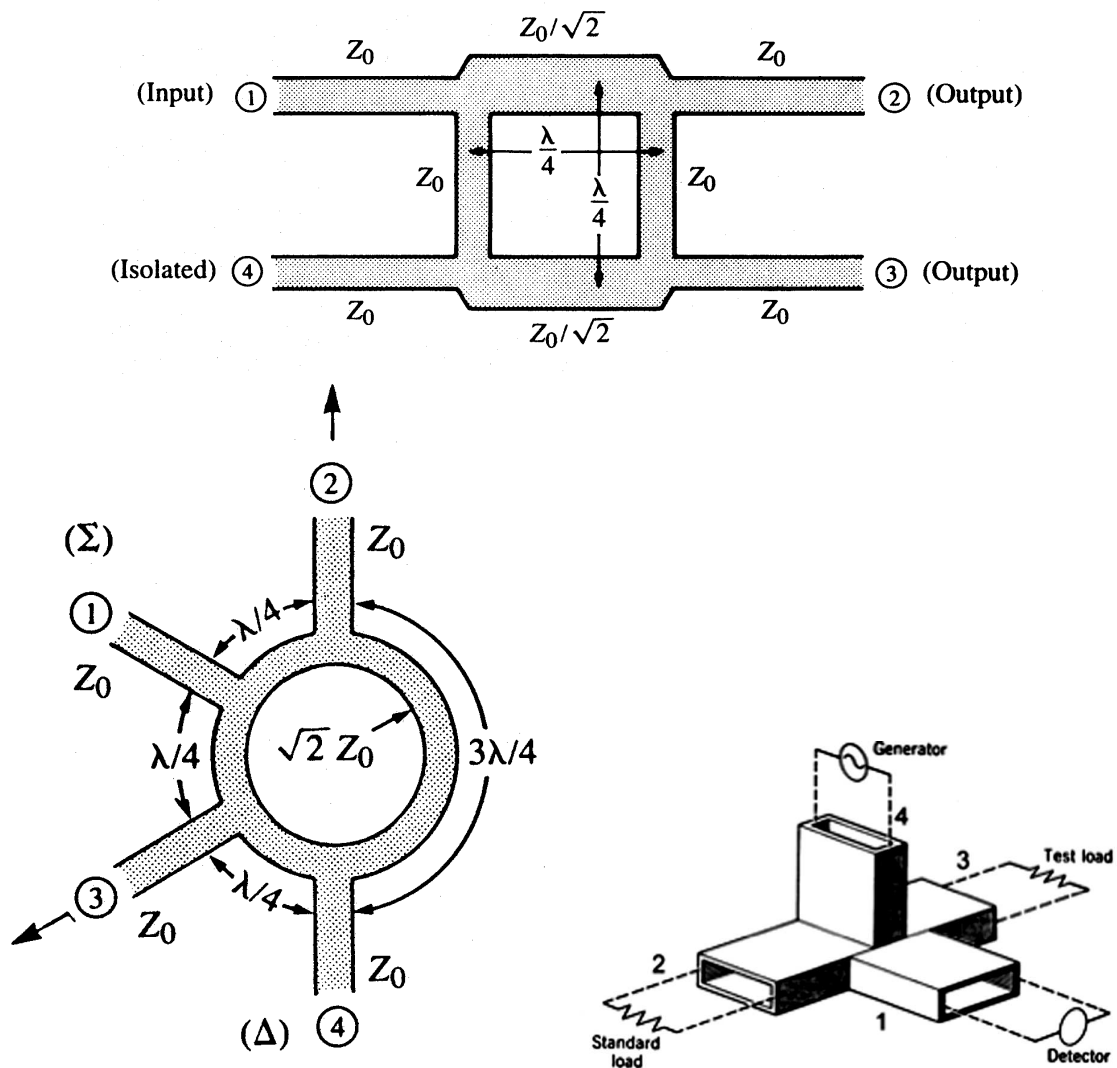


Fig. 12: Top: 90° branch-line coupler; bottom left: 180° ring or rat-race hybrid; bottom right: Magic-T

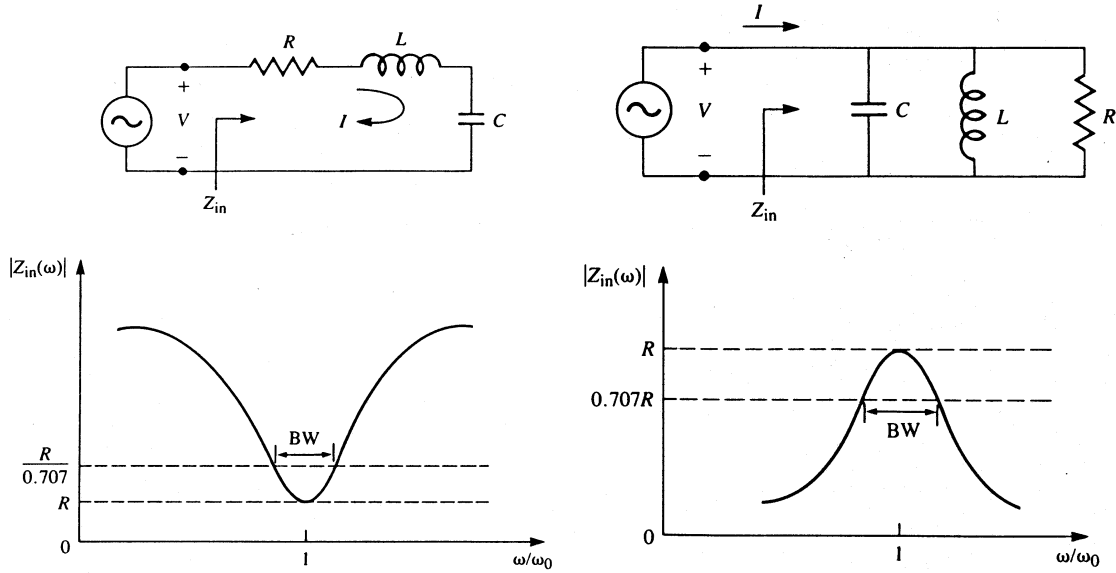


Fig. 13: Left: Series RLC resonator and its response; right: parallel RLC resonator and its response

where

$$P_{loss} = \frac{1}{2} R |i|^2 \quad (80)$$

is the power dissipated in the resistor, and

$$W_m = \frac{1}{4} L |i|^2, \quad W_e = \frac{1}{4} \frac{1}{\omega^2 C} |i|^2 \quad (81)$$

are the average magnetic energy stored in the inductor and the average electric energy stored in the capacitor, respectively. At the **resonance frequency**

$$\omega_0 = \frac{1}{\sqrt{LC}}$$

the stored electric and magnetic energies are equal,  $W_e = W_m$ , and the input impedance is  $Z_{in} = R$ .

A figure of merit of the losses in the circuit is the **quality factor**

$$Q_0 = \omega_0 \frac{W_e + W_m}{P_{loss}} = \frac{\omega_0 L}{R} = \frac{1}{\omega_0 RC} \quad (82)$$

which shows that  $Q_0$  increases if  $R$  decreases.

Close to resonance  $\omega = \omega_0 + \Delta\omega$ , the input impedance (78) can be written as

$$\begin{aligned} Z_{in} &= R + j\omega L \left[ 1 - \frac{1}{\omega^2 LC} \right] = R + j\omega L \frac{\omega^2 - \omega_0^2}{\omega^2} \\ &\approx R + j2L\Delta\omega = R + j2RQ_0 \frac{\Delta\omega}{\omega_0}. \end{aligned} \quad (83)$$

From Eq. (83) we find the **bandwidth B** of the resonator. If  $|Z_{in}|^2 = 2R^2$  the real power delivered to the circuit (79) is one half of that delivered at resonance. The corresponding  $\Delta\omega/\omega_0$  defines the half-bandwidth:

$$\left| R + j 2 R Q_0 \frac{\Delta\omega}{\omega_0} \right|^2 = R^2 \left( 1 + 4 Q_0^2 \left( \frac{\Delta\omega}{\omega_0} \right)^2 \right) = 2 R^2 ,$$

$$2 \Delta\omega/\omega_0 = B = 1/Q_0 . \quad (84)$$

Alternatively to Eq. (83), a resonator with losses can be treated as a lossless resonator whose resonance frequency  $\omega_0$  has been replaced by a complex resonant frequency:

$$\omega_0 \rightarrow \omega_0 \left( 1 + \frac{j}{2Q_0} \right) . \quad (85)$$

The input impedance of a lossless resonator becomes, after substitution of Eq. (85),

$$\begin{aligned} Z_{in} &= j 2 L (\omega - \omega_0) = j 2 L \left( \omega - \omega_0 - j \frac{\omega_0}{2Q_0} \right) \\ &= \omega_0 \frac{L}{Q_0} + j 2 L (\omega - \omega_0) = R + j 2 L \Delta\omega , \end{aligned}$$

which is identical to Eq. (83).

### Parallel circuit

For a parallel circuit the input impedance is

$$Z_{in} = \left( \frac{1}{R} + \frac{1}{j\omega L} + j\omega C \right)^{-1} . \quad (86)$$

$$P_{in} = \frac{1}{2} u i^* = \frac{1}{2} |u|^2 / Z_{in}^* = \frac{1}{2} |u|^2 \left( \frac{1}{R} - \frac{1}{j\omega L} - j\omega C \right) , \quad (87)$$

$$P_{loss} = \frac{1}{2} |u|^2 / R \quad (88)$$

$$W_e = \frac{1}{4} C |u|^2 , \quad W_m = \frac{1}{4} \frac{1}{\omega^2 L} |u|^2 , \quad (89)$$

$$Q_0 = \omega_0 \frac{W_e + W_m}{P_{loss}} = \frac{R}{\omega_0 L} = \omega_0 R C , \quad (90)$$

near resonance,  $\omega = \omega_0 + \Delta\omega$ , the input impedance is given by

$$\begin{aligned} Z_{in} &\approx \left( \frac{1}{R} + \frac{1}{j\omega_0 L} \left( 1 - \frac{\Delta\omega}{\omega_0} \right) + j\omega_0 C + j\Delta\omega C \right)^{-1} \\ &\approx \left( \frac{1}{R} + j\Delta\omega \left( \frac{1}{\omega_0 L} + C \right) \right)^{-1} = \left( \frac{1}{R} + j 2 C \Delta\omega \right)^{-1} \\ &\approx \frac{R}{1 + j 2 Q_0 \Delta\omega/\omega_0} , \end{aligned} \quad (91)$$

$$B = 1/Q_0 . \quad (92)$$

### Loaded $Q$

The above-defined quality factor is characteristic of the circuit itself, i.e. in the absence of any loading effects, and is called **unloaded**  $Q$ . In practice, however, a circuit is inevitably connected to other circuits which will cause additional losses, thus lowering the overall, **loaded**  $Q_l$ . For a series circuit the external load resistor  $R_l$  adds in series with  $R$ , and from (82) follows

$$\frac{1}{Q_l} = \omega_0 C (R + R_l) = \frac{1}{Q_0} + \frac{1}{Q_{ext}} \quad (93)$$

with  $Q_{ext} = 1/\omega_0 R_l C$ .

For a parallel circuit the load resistor is parallel to  $R$  and one obtains from Eq. (90)

$$\frac{1}{Q_l} = \frac{1}{\omega_0 c} \left( \frac{1}{R} + \frac{1}{R_l} \right) = \frac{1}{Q_0} + \frac{1}{Q_{ext}}, \quad (94)$$

with  $Q_{ext} = \omega_0 R_l C$ .

### 4.2 Time response of resonators

In a free-running resonator the dissipated power must equal the rate of change of the stored energy:

$$P_{loss} = -\frac{d}{dt} (W_e + W_m) = -\frac{dW}{dt},$$

which becomes, with the definition of  $Q$  in Eq. (82) or (90),

$$\frac{dW}{dt} = -\frac{\omega_0}{Q} W. \quad (95)$$

Thus, the energy decays exponentially

$$W(t) = W_0 e^{-2t/T_f}, \quad (96)$$

where

$$T_f = 2 Q/\omega_0 \quad (97)$$

is the filling time. Since  $W \sim u^2$  or  $i^2$ , the voltage or current in the circuit decays exactly with  $T_f$ .

As an example, let us consider the parallel circuit in Fig. 13. The source may be an ideal current source, with infinite internal resistance, and delivers a short (compared to the resonance wavelength) pulse of total charge  $q = \int i dt$ . The pulse charges up the capacitor instantaneously (with no current through the inductance) to a voltage  $u_0 = q/C$  and a stored energy  $W_0 = q^2/2C$ . Now, the resonator starts ringing with its resonance frequency  $\omega_0 = 1/\sqrt{LC}$  and the envelope of the voltage decays with  $T_f$ , Eq. (97).

The other extreme is driving the resonator in steady state with a current  $i = i_0 \exp(j \omega t)$ . Then, away from resonance, e.g.  $\omega \ll \omega_0$ , the input impedance (86) is

$$\begin{aligned}
Z_{in} &= R \left( 1 - j \frac{R}{\omega L} + j \omega R C \right)^{-1} \\
&= R \left( 1 - j Q_0 \frac{\omega_0}{\omega} + j Q_0 \frac{\omega}{\omega_0} \right)^{-1} \\
&\approx R / (1 - j Q_0 \omega_0 / \omega) \\
&\approx j \frac{R}{Q_0} \frac{\omega}{\omega_0} \ll j R,
\end{aligned} \tag{98}$$

and the voltage is small and inductive. Near resonance, the impedance is given by Eq. (91) and the voltage is

$$u = \frac{R i_0}{1 + j 2 Q_0 \Delta\omega / \omega_0} e^{j\omega t}, \tag{99}$$

i.e. it is  $R i_0$  at resonance and decays fast off-resonance (for large- $Q$  circuits). At  $\omega_0$  it changes from a positive to a negative phase. The full behaviour is shown in Fig. 14.

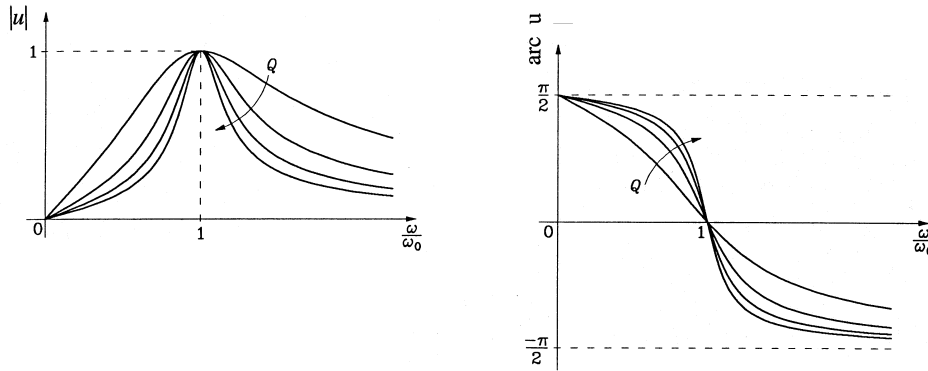


Fig. 14: Magnitude and phase of the voltage across a parallel resonance circuit

Equation (99) shows a phase difference  $\Delta\varphi$  between the driving current and the resonator voltage of

$$\tan \Delta\varphi = -2 Q_0 \frac{\Delta\omega}{\omega_0}. \tag{100}$$

This phase difference is zero at resonance and  $\mp 45^\circ$  for  $\Delta\omega = \pm B/2$ .

As a last example we consider the switching on of a harmonic current with frequency  $\omega_0$ :

$$i(t) = \begin{cases} 0 & \text{for } t \leq 0 \\ i_0 \sin \omega_0 t & \text{for } t > 0. \end{cases} \tag{101}$$

The differential equation of the circuit is

$$i(t) = \frac{1}{R} u(t) + \frac{1}{L} \int u(t) dt + C \frac{du(t)}{dt}. \tag{102}$$

We apply the Laplace transform and obtain

$$\frac{1}{C} \frac{\omega_0}{s^2 + \omega_0^2} i_0 = \frac{2}{T_f} U(s) + \omega_0^2 \frac{1}{s} U(s) + s U(s)$$

or, after solving for  $U(s)$ ,

$$U(s) = \frac{s}{s^2 + \omega_0^2} \cdot \frac{1}{s^2 + 2s/T_f + \omega_0^2} \cdot \frac{\omega_0}{C} i_0.$$

After decomposing the right side into partial fractions,

$$U(s) = \left[ \frac{\omega_0}{s^2 + \omega_0^2} - \frac{\omega_0}{s^2 + 2s/T_f + \omega_0^2} \right] R i_0,$$

the inverse Laplace transform gives

$$u(t) = \left\{ \sin \omega_0 t - \frac{\exp(-t/T_f)}{\sqrt{1 - 1/4Q_0^2}} \sin \left( \omega_0 \sqrt{1 - 1/4Q_0^2} t \right) \right\} R i_0,$$

which for high  $Q$ -values can be written as

$$u(t) \approx \left\{ \left( 1 - e^{-t/T_f} \right) \sin \omega_0 t + \frac{t}{4T_f} e^{-t/T_f} \cos \omega_0 t \right\} R i_0. \quad (103)$$

In deriving Eq. (103) we put  $\cos(t/4T_f) \approx 1$  and  $\sin(t/4T_f) \approx t/4T_f$ , since these terms will vanish owing to the exponential for large values of  $t/T_f$ .

As can be seen from Eq. (103) the resulting voltage consists of a transient part, which decays exponentially, and the steady-state part, given by Eq. (99) for  $\Delta\omega = 0$ .

### 4.3 Transmission-line resonator

The most simple microwave resonator is one made of a transmission line. It is also an arrangement which allows for the study of the filling of a resonator with microwave energy in a very intuitive way.

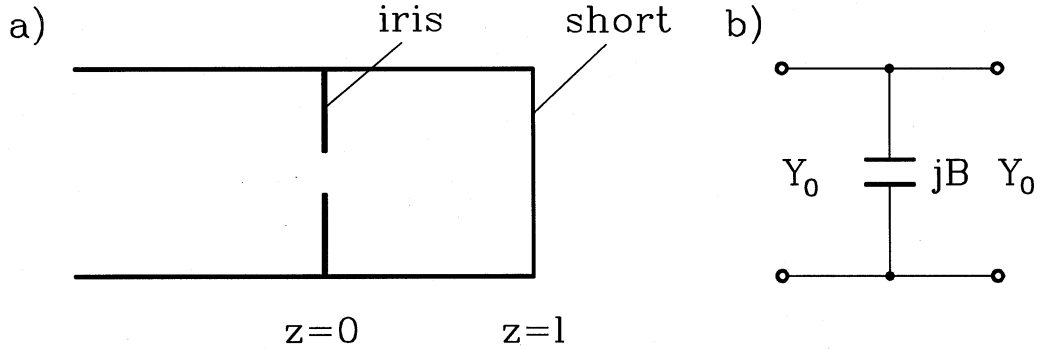


Fig. 15: (a) Shorted transmission line with iris; (b) equivalent circuit of a thin lossless iris parallel to electric fields

Let us consider a shorted transmission line with an iris a distance  $l$  away from the short, see Fig. 15(a). If the mode on the line is such that the electric fields are parallel to the iris, the iris will concentrate the electric fields and electric energy will be stored around the iris. Then, if we assume negligible losses and a thin iris, the iris can be represented as a lumped capacitance, Fig. 15(b). The value of  $B$  has to be



computed with field theoretical means and will not be derived here. The interested reader will find it in Vol. 10 of Ref. [2]. Such an iris in an infinitely long transmission line causes a reflection, Eq. (23), of

$$r = \frac{Z_e - Z_0}{Z_e + Z_0} = \frac{Y_0 - Y_e}{Y_0 + Y_e} = \frac{-jB}{2Y_0 + jB} \quad (104)$$

and has a transmission (see also Vol. 10 of Ref. [2]) of

$$t = 1 + r. \quad (105)$$

Now, we turn on the RF and launch a wave down the line, toward the structure formed by the iris and the short, as seen in Fig. 16. For a small iris opening one expects that most of the wave will be reflected. Some will be transmitted through the iris. The transmitted part travels to the short, is reflected, returns to the iris, where it radiates a little bit through, but most of it is reflected. With time, and if the phases are right, the fields build up in the resonator. In steady state the incoming reflected wave interferes destructively with the radiation from the cavity, and if the coupling of the iris and the dissipation in the cavity are in a ‘matched’ condition the reflection disappears.

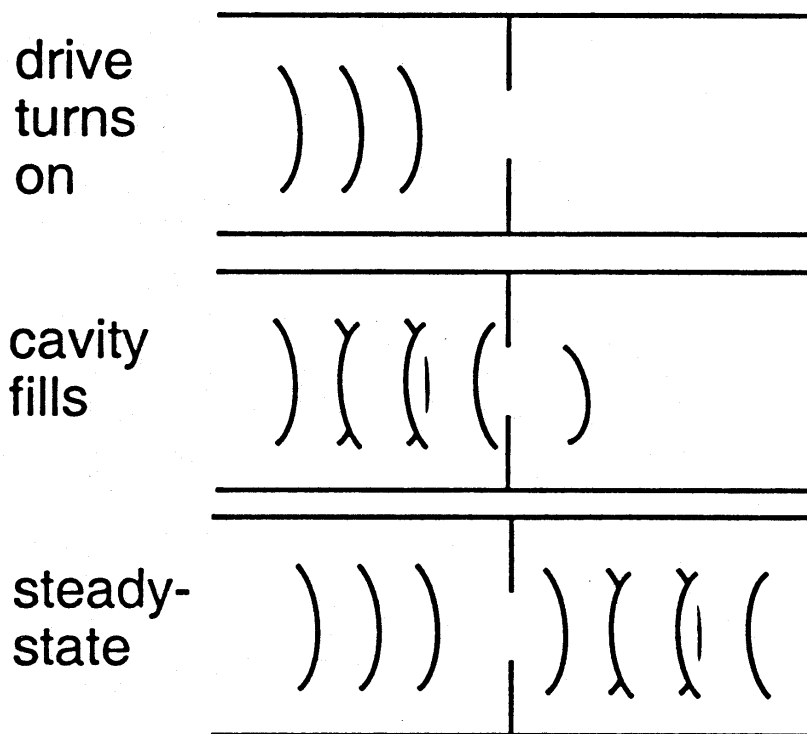


Fig. 16: Illustration of the filling of the cavity of Fig. 15

The process can be calculated in a step-by-step approach. The incident wave with complex amplitude  $a$  is reflected by the iris with value  $ra$ , while a fraction  $ta$  is transmitted. This wave travels to the short in a time  $\tau = l/v_g$ , where  $v_g$  is the group velocity in the unloaded line, is reflected with  $r_s = -1$  and returns to the iris, where it is reflected and partially transmitted, and so on. Mathematically we find for the wave on the right side of the iris and travelling to the right

$$a_+ = ta - r e^{-2\gamma l} ta + (r e^{-2\gamma l})^2 ta - (r e^{-2\gamma l})^3 ta \pm \dots = \frac{ta}{1 + r e^{-2\gamma l}}. \quad (106)$$

Similarly, we find for the wave on the left side of the iris and travelling to the left

$$\begin{aligned}
 a_- &= r a - e^{-2\gamma l} t^2 a + r e^{-4\gamma l} t^2 a - r^2 e^{-6\gamma l} t^2 a \pm \dots \\
 &= r a - e^{-2\gamma l} \left[ 1 - r e^{-2\gamma l} + (r e^{-2\gamma l})^2 \mp \dots \right] t^2 a \\
 &= \left[ r - \frac{t^2 e^{-2\gamma l}}{1 + r e^{-2\gamma l}} \right] a = \frac{r + (r^2 - t^2) e^{-2\gamma l}}{1 + r e^{-2\gamma l}} a.
 \end{aligned} \tag{107}$$

Making use of Eq. (105) the condition for zero reflection in steady state is

$$r = \frac{e^{-2\gamma l}}{1 - 2 e^{-2\gamma l}}, \tag{108}$$

which, substituted into Eq. (106), yields

$$a_+ = \frac{1 + r}{1 + r e^{-2\gamma l}} a = \frac{a}{1 - e^{-2\gamma l}}. \tag{109}$$

The admissible parameter space which satisfies Eqs. (108) and (109) and the requirement  $|r| < 1$  can be shown graphically (Fig. 17). For given losses  $2\alpha l$  the dashed segment indicates the area where  $|r|$  would be larger than one. Any  $2\beta l$  larger than  $(2\beta l)_c$  is allowed. The inverse of the magnitude of the phasor  $\tilde{p}$  gives then the build-up factor  $|a_+/a|$  in the resonator.

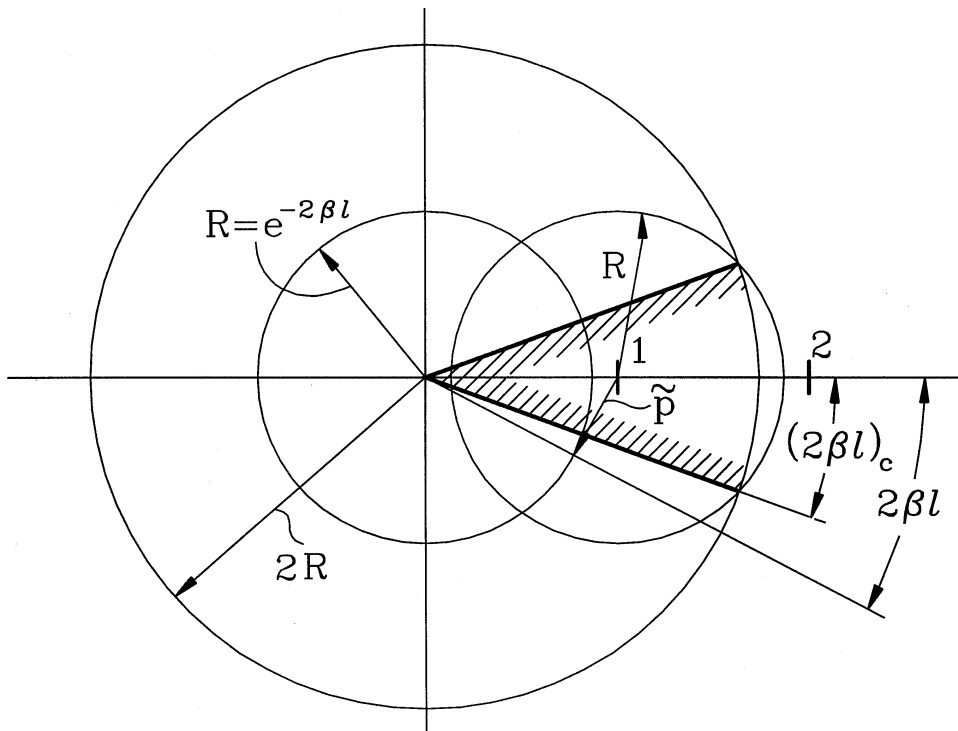


Fig. 17: Graphical solution of Eqs. (108) and (109). Any  $2\beta l > (2\beta l)_c$  is admissible; admissible parameter  $> (2\beta l)_c \cdot |\tilde{p}|^{-1}$  gives the field build-up in the resonator.

#### 4.4 Cavity-resonator parameters

Cavity resonators for acceleration are basically characterized by four parameters:

- The resonant frequency  $\omega_0$ .
- The  $Q$ -value.
- The  $R$  upon  $Q$ , which is a measure for providing an accelerating voltage  $V_0$  with a certain stored energy  $W$ :

$$\frac{R}{Q} = \frac{V_0^2}{\omega_0 W}. \quad (110)$$

- The **shunt impedance**  $R$ , which measures the efficiency to create an accelerating voltage  $V_0$  with a certain dissipated power  $P_d$ :

$$R = \frac{V_0^2}{P_d}. \quad (111)$$

Note that sometimes the definition  $R = V_0^2/2P_d$  is used, where the factor 2 is inserted for similarity with a peak a.c. voltage  $V_0$  at a resistor  $R$ .

The accelerating voltage is given by the integration of the accelerating field over a typical length  $L$ :

$$V_0 = \int_0^L E(z, t(z)) dz, \quad (112)$$

where  $t(z)$  is the time at which a particle is at location  $z$ , i.e.  $t(z) = \int dz/\nu(z) + t_0$  and  $t_0$  has to be chosen such that  $V_0$  becomes maximum.

To illustrate Eq. (112) we take the example of a closed cylindrical cavity of length  $g$  which is driven in the  $TM_{010}$  mode, Fig. 18. The electric field is parallel to the cavity axis and is independent of  $z$ :

$$\mathbf{E} = E_0 \cos \omega_0 t \mathbf{e}_z.$$

Then, the accelerating voltage for a particle with constant speed  $\nu$  is given by

$$\begin{aligned} V_0 &= \max_{t_0} \left\{ E_0 \int_0^g \cos[\omega_0(z/\nu + t_0)] dz \right\} \\ &= E_0 \max_{t_0} \left\{ \frac{\nu}{\omega_0} [\sin \omega_0(g/\nu + t_0) - \sin \omega_0 t_0] \right\}, \end{aligned}$$

which is maximum for  $\omega_0 t_0 = -\omega_0 g/2\nu$  and has the value

$$V_0 = E_0 g T, \quad T = \sin \left( \frac{\omega_0 g}{2\nu} \right) / \left( \frac{\omega_0 g}{2\nu} \right). \quad (113)$$

$T$  is the **transit time factor** and takes into account the change of  $E$  with time while the particle traverses the cavity gap.

Often, instead of a single accelerating gap, there is a chain of cavities each of length  $L$ . Then, the parameters (110) and (111) are given per unit length:

$$\begin{aligned}
 R' &= \frac{E_0^2}{P_d'}, \\
 E_0 &= V_0/L, \\
 (R/Q)' &= \frac{E_0^2}{\omega_0 W'}.
 \end{aligned}
 \tag{114}$$

The shunt impedance is a key parameter because it determines the accelerating voltage available from a given input power  $P_{in} = P_d$ , if the cavity is not loaded by a beam. The  $R$  upon  $Q$ , on the other hand, is independent of the material losses and depends only on the cavity mode and geometry. It measures how much stored energy is required for the wanted accelerating voltage.

One mode in a cavity resonator can be modelled by an equivalent circuit, as in Fig. 13. In the case of the parallel circuit, for instance, the gap voltage  $V_0$  would be across the capacitor and the circuit parameters follow from the cavity parameters as

$$\begin{aligned}
 R_{circuit} &= \frac{1}{2} R, \\
 C_{circuit} &= \frac{2}{\omega_0 R/Q}, \\
 L_{circuit} &= \frac{1}{2\omega_0} \frac{R}{Q}.
 \end{aligned}
 \tag{115}$$

Finally, let us calculate the cavity parameters for a simple example, namely for the  $TM_{010}$  mode in a closed cylindrical cavity, Fig. 18. This is a good approximation for a cavity with small beam pipes and is the most standard configuration.

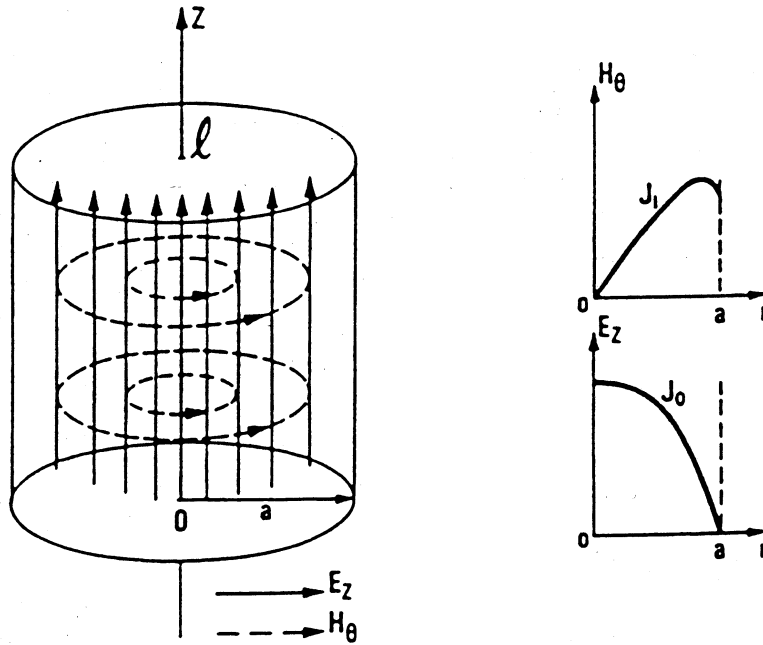


Fig. 18:  $TM_{010}$  mode in a pill-box cavity

The field components are

$$\begin{aligned}
E_z &= E_0 J_0(j_{01} \rho/a), \\
Z_0 H_\varphi &= j J_1(j_{01} \rho/a), \\
Z_0 &= \sqrt{\mu_0/\varepsilon_0},
\end{aligned} \tag{116}$$

where  $a$  is the cavity radius and  $j_{01}$  is the first zero of the zero-order Bessel function.

The stored energy in the cavity is

$$\begin{aligned}
W &= W_{mag} + W_{el} = 2 W_{el} = 2 \frac{\varepsilon_0}{4} \int_0^a \int_0^{2\pi} \int_{-g/2}^{g/2} E_0^2 J_0^2(j_{01} \frac{\rho}{a}) \rho d\rho d\varphi dz \\
&= \frac{\varepsilon_0}{2} 2\pi g a^2 E_0^2 \int_0^1 x J_0^2(j_{01} x) dx \\
&= \frac{\pi}{2} \varepsilon_0 E_0^2 g a^2 J_1^2(j_{01}).
\end{aligned} \tag{117}$$

The losses are calculated by means of the power-loss method, that is from the wall currents of the ideal conducting cavity:

$$\begin{aligned}
P_d &= \frac{1}{2\kappa\delta} \left\{ 2 \int_0^a |H_\varphi(z=0)|^2 2\pi\rho d\rho + \int_{-g/2}^{g/2} |H_\varphi(\rho=a)|^2 2\pi a dz \right\} \\
&= \frac{\pi}{\kappa\delta} \frac{\varepsilon_0}{\mu_0} E_0^2 \left\{ 2a^2 \int_0^1 J_1^2(j_{01} x) x dx + ag J_1^2(j_{01}) \right\} \\
&= \frac{\pi}{\kappa\delta} \left( \frac{E_0}{Z_0} \right)^2 a(a+g) J_1^2(j_{01}),
\end{aligned} \tag{118}$$

where  $\delta = 2(\omega\mu_0\kappa)^{1/2}$  is the skin depth.

The cavity voltage is given in Eq. (113). Then, shunt impedance,  $Q$ -value and frequency become

$$\begin{aligned}
R &= \frac{V^2}{P_d} = \frac{1}{\pi} \kappa \delta Z_0^2 \frac{(g/a)^2 \sin kg/2}{1+g/a} \frac{1}{J_1^2(j_{01})} \\
k &= \omega/c_0, \\
Q_0 &= \frac{\omega w}{P_d} = \frac{1}{\delta} \frac{g}{1+g/a}, \\
f &= \frac{j_{01} c}{2\pi a}.
\end{aligned} \tag{119}$$

For a 3 GHz copper cavity with a gap of half a wavelength the values are:

$$\begin{aligned}
j_{01} &= 2.405, & J_1(j_{01}) &= 0.5191 & \kappa &= 58 \times 10^6 \Omega^{-1} \text{ m}^{-1}, \\
a &= 3.828 \text{ cm}, & g &= 5 \text{ cm}, & \delta &= 1.207 \mu\text{m}, \\
T &= \frac{\sin kg/2}{kg/2} = \frac{2}{\pi} & & & & \text{transit time factor,}
\end{aligned}$$

$$R' = R/g = 100 \text{ M}\Omega/\text{m}, \quad Q_0 = 17963, \quad R'/Q_0 = 6.1 \text{ k}\Omega/\text{m}, \quad T_0 = \frac{2Q_0}{\omega} = 1.9 \mu\text{s}.$$

#### 4.5 Cavity shape perturbation

Inserting small metallic objects into a cavity or slightly deforming the shape of the cavity can be treated by the perturbation technique [4], [5].

Let us designate the fields and the resonant frequency of the unperturbed cavity by  $\mathbf{E}_0, \mathbf{H}_0, \omega_0$  and of the perturbed cavity by  $\mathbf{E}, \mathbf{H}, \omega$ ; then Maxwell's equations are

$$\nabla \times \mathbf{E}_0 = -j\omega_0 \mu \mathbf{H}_0, \quad \nabla \times \mathbf{H}_0 = j\omega_0 \varepsilon \mathbf{E}_0, \quad (120)$$

$$\nabla \times \mathbf{E} = -j\omega \mu \mathbf{H}, \quad \nabla \times \mathbf{H} = j\omega \varepsilon \mathbf{E}, \quad (121)$$

Manipulating Eqs. (120) and (121) we find

$$\begin{aligned} \mathbf{H} \cdot (\nabla \times \mathbf{E}_0^*) - \mathbf{E}_0^* \cdot (\nabla \times \mathbf{H}) &= \nabla \cdot (\mathbf{E}_0^* \times \mathbf{H}) = j\omega_0 \mu \mathbf{H} \cdot \mathbf{H}_0^* - j\omega \varepsilon \mathbf{E}_0^* \cdot \mathbf{E}, \\ \mathbf{H}_0^* \cdot (\nabla \times \mathbf{E}) - \mathbf{E} \cdot (\nabla \times \mathbf{H}_0^*) &= \nabla \cdot (\mathbf{E} \times \mathbf{H}_0^*) = -j\omega \mu \mathbf{H}_0^* \cdot \mathbf{H} + j\omega_0 \varepsilon \mathbf{E} \cdot \mathbf{E}_0^*, \end{aligned}$$

and after adding both equations and integration over the volume  $V$  of the perturbed cavity

$$\begin{aligned} \int_V \nabla \cdot (\mathbf{E} \times \mathbf{H}_0^* + \mathbf{E}_0^* \times \mathbf{H}) dV &= \oint_S (\mathbf{E} \times \mathbf{H}_0^* + \mathbf{E}_0^* \times \mathbf{H}) d\mathbf{S} \\ &= \oint_S (\mathbf{E}_0^* \times \mathbf{H}) \cdot d\mathbf{S} = -j(\omega - \omega_0) \int_V (\varepsilon \mathbf{E} \cdot \mathbf{E}_0^* + \mu \mathbf{H} \cdot \mathbf{H}_0^*) dV. \end{aligned} \quad (122)$$

In deriving Eq. (122) we used Gauss' theorem and the fact that  $\mathbf{n} \times \mathbf{E} = 0$  on the surface  $S$  of the perturbed cavity. Referring to Fig. 19, we see that  $S = S_0 - \Delta S$  and write for the left side of Eq. (122)

$$\oint_S (\mathbf{E}_0^* \times \mathbf{H}) d\mathbf{S} = \oint_{S_0} (\mathbf{E}_0^* \times \mathbf{H}) d\mathbf{S} - \oint_{\Delta S} (\mathbf{E}_0^* \times \mathbf{H}) d\mathbf{S} = - \int_{\Delta S} (\mathbf{E}_0^* \times \mathbf{H}) d\mathbf{S},$$

because  $\mathbf{n} \times \mathbf{E}_0 = 0$  on  $S_0$ . Substitution into Eq. (122) gives

$$\omega - \omega_0 = -j \frac{\oint_{\Delta S} (\mathbf{E}_0^* \times \mathbf{H}) d\mathbf{S}}{\int_V (\varepsilon \mathbf{E} \cdot \mathbf{E}_0^* + \mu \mathbf{H} \cdot \mathbf{H}_0^*) dV}. \quad (123)$$

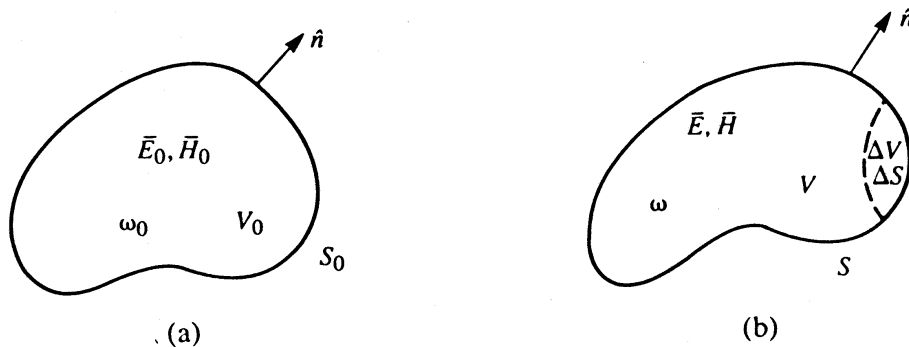


Fig. 19: Resonant cavity perturbed by a change in shape: (a) original cavity; (b) perturbed cavity

Equation (123) is the exact expression for the change in the resonant frequency. However, it is of little use since we do not know the quantities  $\mathbf{E}$ ,  $\mathbf{H}$  of the perturbed cavity. But if the perturbation is small,  $\mathbf{E}$ ,  $\mathbf{H}$  can be replaced by  $\mathbf{E}_0$ ,  $\mathbf{H}_0$  in the denominator of Eq. (123) because it is essentially the stored energy in the cavity and this will not change much. In the numerator we approximate  $\mathbf{H}$  by  $\mathbf{H}_0$  and use Poynting's theorem,

$$\oint_{\Delta S} (\mathbf{E}_0^* \times \mathbf{H}) d\mathbf{S} \approx \oint_{\Delta S} (\mathbf{E}_0^* \times \mathbf{H}_0) d\mathbf{S} = -j\omega_0 \int_{\Delta V} (\varepsilon |\mathbf{E}_0|^2 - \mu |\mathbf{H}_0|^2) dV,$$

which finally gives for Eq. (123)

$$\frac{\omega - \omega_0}{\omega_0} \approx \frac{\int_{\Delta V} (\mu |\mathbf{H}_0|^2 - \varepsilon |\mathbf{E}_0|^2) dV}{\int_{V_0} (\mu |\mathbf{H}_0|^2 + \varepsilon |\mathbf{E}_0|^2) dV} = \frac{\Delta W_m - \Delta W_e}{W_m + W_e}. \quad (124)$$

The terms  $\Delta W_m$ ,  $\Delta W_e$  are the changes in the stored magnetic and electric energy, respectively, and  $W_m + W_e$  is the total stored energy. The result shows that the frequency may either increase or decrease depending on the location and the character of the perturbation.

The formula (124) was derived by pushing the cavity wall inwards by a small amount. It seems reasonable to suppose that introducing a small metallic object into the interior of the cavity should perturb the frequency in a similar way by an amount depending upon the local fields, and thus we could use the frequency shift to measure the field strength at an interior point. This is in fact the case. We might further suppose that we only have to perform the integration of the unperturbed fields over the volume of the perturbing object. This, however, is far from the case because the object perturbs the field in a way that is essential. In order to calculate the field perturbation we follow a procedure for a small metallic sphere as outlined in Ref. [6]. With the well-known electric field of a metallic sphere in a homogeneous electrostatic field the volume integral over the electric field was performed when changing the sphere radius from  $r_0$  to  $r_0 + dr_0$ . For the total perturbation caused by the sphere of radius  $r_0$  the resulting expression was integrated from zero to  $r_0$ . In an analogous manner the volume integral over the magnetic field was carried out. As a result form factors for the volume integrals in the numerator of Eq. (124) were found:

$$f_e = 3/2, \quad f_m = 3/4.$$

In general, these form factors depend on the shape and orientation and material of the perturbing object. For some geometries, like ellipsoids, they are calculated [6]; for other more complicated geometries they can be determined experimentally [7].

## 5 MEASUREMENTS

Measurement techniques are a vast and complicated area. Here, I present a few basic techniques directly related to the subjects treated in the previous section.

### 5.1 Line mismatch

An old-fashioned but instructive way to measure a line mismatch is with a slotted line, Fig. 20. A movable capacitive probe measures the voltage standing wave ratio, Eq. (33), along the mismatched line. This yields the magnitude of the reflection coefficient. We further know from Section 2.3 that the first voltage minimum occurs at a distance  $\zeta_{\min}$  from the load

$$2\beta \zeta_{\min} = \vartheta - \pi$$

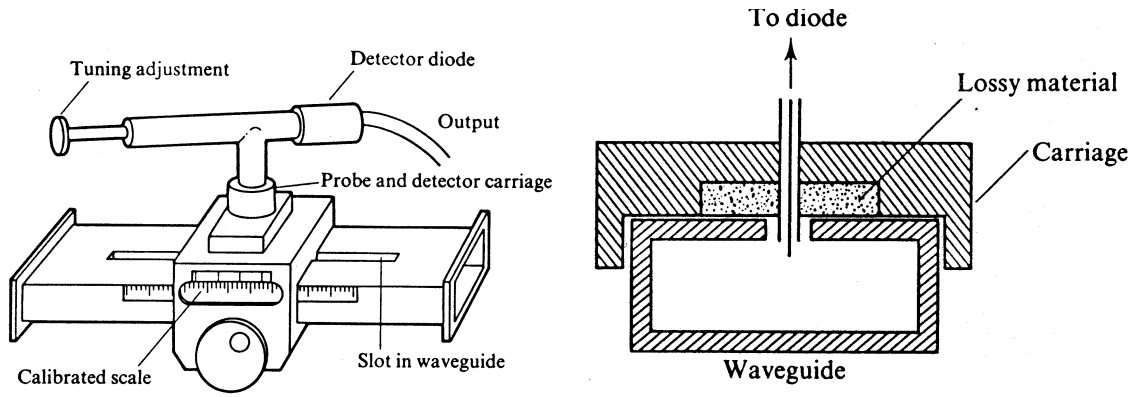


Fig. 20: Standing wave detector: left: complete device with slotted rectangular waveguide; right: probe in waveguide

which fixes the phase  $\vartheta$  of the reflection coefficient.

An alternative solution for measuring the magnitude of the reflection coefficient is shown in Fig. 21. A fraction of the forward- and backward-travelling power is coupled out by two directional couplers, giving the measurements shown.

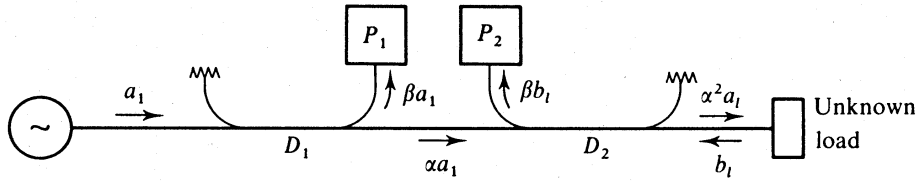


Fig. 21: Measurement of the ratio of backward ( $P_2$ ) to forward ( $P_1$ ) travelling power with two directional couplers  $D_1$ ,  $D_2$ .

## 5.2 $Q$ -value and coupling factor of a cavity [8]

Let us consider a cavity coupled to a signal generator via a piece of a transmission line and a coupling device. The source has an internal impedance  $Z_0$  equal to the line impedance. The equivalent circuits are shown in Fig. 22.  $L_1$  represents the self-inductance of the coupling device and  $M$  the mutual inductance between it and the cavity inductance  $L$ . The terminal plane of the coupling device is presumed to be located at some arbitrary position a–a near the cavity. The coupling device is assumed to be lossfree. The circuit can be simplified further as shown on the right of Fig. 22.

The normalized impedance at the terminal plane a–a is then

$$\begin{aligned} \frac{Z_{aa}}{Z_0} &= j \frac{X_1}{Z_0} + \frac{1}{Z_0} \frac{(\omega M)^2}{R_s + j(\omega L_1/\omega C)} \\ &= j \frac{X_1}{Z_0} + \frac{\beta_1}{1 + j(\omega L/R_s)[1 - (\omega_0/\omega)^2]} \approx j \frac{X_1}{Z_0} + \frac{\beta_1}{1 + j2Q_0\delta}, \end{aligned} \quad (125)$$

where  $X_1 = \omega L_1$ ,  $\beta_1 = (\omega M)^2/Z_0 R_s$ ,  $\delta = (\omega - \omega_0)/\omega$ .

The analysis can be simplified by shifting the reference plane to a location where the term with  $X_1$  vanishes. Such a location is called the **detuned-short position** because a short circuit will appear if the resonator impedance is far off-resonance. We find the detuned-short position by transforming the impedance  $Z_{aa}$  with a piece of line of length  $l$ . From Eq. (35) follows



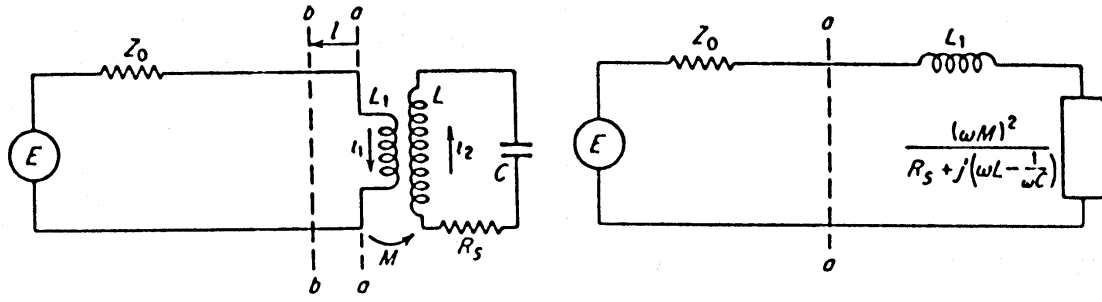


Fig. 22: Cavity coupled to a generator through a line; left: equivalent circuit; right: equivalent circuit with the impedances referred to the primary

$$\frac{Z_{bb}}{Z_0} = \frac{Z_{aa} + j Z_0 \tan \beta l}{Z_0 + j Z_{aa} \tan \beta l}, \quad (126)$$

which is zero at

$$\tan \beta l = j \frac{Z_{aa}}{Z_0} = -\frac{X_1}{Z_0} \quad \text{for} \quad \frac{Z_{aa}}{Z_0} = j \frac{X_1}{Z_0}. \quad (127)$$

Substituting Eqs. (125) and (127) into (126) gives the simple expression for the impedance at the detuned-short position:

$$\frac{Z_{bb}}{Z_0} = \frac{\beta}{1 + j2Q_0(\delta - \delta_0)}, \quad (128)$$

with

$$\beta = \frac{\beta_1}{1 + (X_1/Z_0)^2}, \quad \delta_0 = \frac{\beta}{2Q_0} \frac{X_1}{Z_0}, \quad \beta_1 = \frac{(\omega M)^2}{Z_0 R_s}.$$

Equation (128) represents the impedance of a parallel resonant circuit with a resonant impedance  $\beta Z_0$ . In the Smith chart, Fig. 23, it is a circle with the centre located on the real axis and touching the point  $r = R/Z_0 = 0$ . At resonance the circle cuts the real axis at the point  $r_0 = \beta$ . This determines the coupling coefficient. If

$$r_0 = \beta \begin{cases} < 1 \\ = 1 \\ > 1 \end{cases} \quad \text{the resonator is} \begin{cases} \text{undercoupled} \\ \text{matched} \\ \text{overcoupled} \end{cases} \quad \text{with} \quad Q_{ext} \begin{cases} > Q_0 \\ = Q_0 \\ < Q_0 \end{cases}.$$

At certain frequencies the imaginary part of the denominator becomes equal to  $\pm 1$ , then

$$\frac{Z_{bb}}{Z_0} = \frac{\beta}{1 \pm j},$$

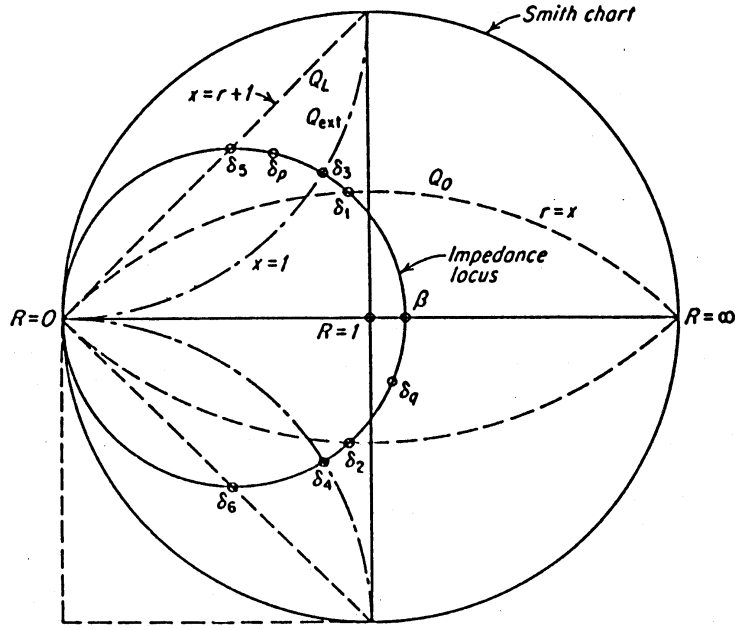


Fig. 23: Identification of the half-power points from the Smith chart. The  $Q_0$  locus is given by  $x = r$ ;  $Q_l$  by  $x = 1 + r$ ;  $Q_{ext}$  by  $x = 1$ .

and the real part of  $Z_{bb}$  equals the imaginary part. The locus of these points is the dashed segments ( $r = x$ ) in Fig. 23. They cut the impedance circle at frequencies  $\delta_1$  and  $\delta_2$  and determine the unloaded  $Q$ :

$$\begin{aligned} 2Q_0(\delta_1 - \delta_0) &= 1 \\ 2Q_0(\delta_2 - \delta_0) &= -1 \end{aligned} \Rightarrow Q_0 = \frac{1}{\delta_1 - \delta_2}. \quad (129)$$

The coupling coefficient  $\beta$  is also the ratio of the power radiated from the resonator into the external circuit to the power dissipated in the resonator

$$\beta = \frac{P_{ext}}{P_d} = \frac{Q_0}{Q_{ext}}. \quad (130)$$

Eq. (130) together with Eq. (93) gives for the loaded  $Q$

$$\frac{1}{Q_l} = \frac{1}{Q_0} + \frac{1}{Q_{ext}} = \frac{1}{Q_0} + \frac{1}{Q_0} \frac{Q_0}{Q_{ext}}$$

or

$$Q_l = \frac{Q_0}{1 + \beta}, \quad Q_{ext} = \frac{Q_0}{\beta}. \quad (131)$$

We write Eq. (128) in terms of  $Q_l$  and  $Q_{ext}$ ,

$$\frac{Z_{bb}}{Z_0} = \frac{\beta}{1 + j2Q_l(1 + \beta)(\delta - \delta_0)} = \frac{\beta}{1 + j2Q_{ext}\beta(\delta - \delta_0)},$$

and see that for frequencies  $\delta_5, \delta_6$  at which

$$2Q_l(\delta - \delta_0) = \pm 1 \quad \text{or} \quad Q_l = 1/(\delta_5 - \delta_6) \quad (132)$$

the impedance is

$$\frac{Z_{bb}}{Z_0} = \frac{\beta}{1 \pm j(1 + \beta)} + \frac{1}{1/\beta \pm j(1 + 1/\beta)}.$$

The locus of these points is  $x = 1 + r$  and is given by straight lines in Fig. 23. They cut the impedance circle at frequencies  $\delta_5$  and  $\delta_6$  and determine the loaded  $Q_l$ . Finally, for frequencies  $\delta_3, \delta_4$  at which

$$2Q_{ext}(\delta - \delta_0) = \pm 1 \quad \text{or} \quad Q_{ext} = 1/(\delta_3 - \delta_4) ,$$

the impedance is

$$\frac{Z_{bb}}{Z_0} = \frac{\beta}{1 \pm j\beta} = \frac{1}{1/\beta \pm j}.$$

with the locus of the points given by  $x = 1$  (dot-dashed line in Fig. 23). The intersections with the impedance circle determine  $\delta_3, \delta_4$  and thus  $Q_{ext}$ .

### 5.3 $R$ upon $Q$ of a cavity [5], [9]

The measurement of the resonant frequency and  $Q$ -value of a cavity is relatively easy. More difficult is the measurement of the shunt impedance. We use the definition of the  $R$  upon  $Q$ , Eq. (110), for a standing wave cavity where the electric field is proportional to  $\exp(j\omega t)$ . Then, Eq. (110), together with Eq. (112), is equivalent to

$$\frac{R}{Q} = \frac{1}{\omega_0 W} \left| \int E_z(z) e^{j\omega t} dz \right|^2 = \frac{1}{\omega_0 W} \left| \int E_z(z) e^{jkt} dz \right|^2.$$

for a relativistic,  $\nu \approx c$ ,  $k = \omega/c$ , particle. This can be written as

$$\frac{R}{Q} = \frac{1}{2\pi f_0 W} \left\{ \left( \int E_z \cos kz dz \right)^2 + \left( \int E_z \sin kz dz \right)^2 \right\}. \quad (133)$$

Next, we make use of the perturbation formula Eq. (124) where we choose a trajectory with zero magnetic field,  $H_0 = 0$ , and where we write the integral over the perturbed electric field with the aid of a form factor  $K_e$ :

$$\frac{\Delta\omega}{\omega_0} = \frac{1}{4W} K_e \varepsilon E_0^2. \quad (134)$$

The term  $K_e$  depends on the material, size, and shape of the perturbing object (bead). Since  $E_0$  is a function of the position  $z$ ,  $\Delta\omega = \Delta\omega(z)$ . Identifying  $E_0$  in Eq. (134) as being the accelerating field  $E_z$  in Eq. (133), we get after substitution

$$\frac{R}{Q} = \frac{2}{\pi f_0 K_e \varepsilon} \left\{ \left( \int \sqrt{\frac{\Delta\omega(z)}{\omega_0}} \cos kz dz \right)^2 + \left( \int \sqrt{\frac{\Delta\omega}{\omega_0}} \sin kz dz \right)^2 \right\}. \quad (135)$$

Therefore the problem is reduced to the measurement of the frequency shifts  $\Delta\omega/\omega$  as a function of the position  $z$  of the perturbing object. Instead of the frequency shift it is easier to measure the phase shift of the signal which is related to the frequency shift by (see Eq. (99))

$$\tan \varphi = 2Q_l \frac{\Delta\omega}{\omega_0}. \quad (136)$$

A set-up to measure the phase shift with a network analyser is shown in Fig. 24. The perturbing bead is pulled through the cavity by a stepping motor while the network analyser continuously measures the phase.

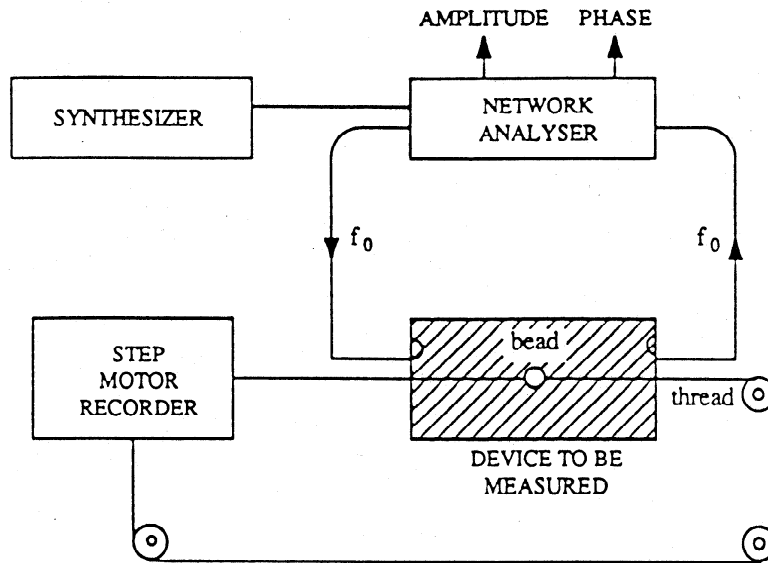


Fig. 24: Bead-pull measurement set-up for measuring the  $R$  upon  $Q$  of a cavity

## REFERENCES

- [1] J.C. Maxwell, *A Treatise on Electricity and Magnetism* (Dover, New York, 1954).
- [2] Radiation Laboratory Series, Massachusetts Institute of Technology, McGraw-Hill, New York: CD-ROM published by Artech House, Norwood, 1999.
- [3] S. Ramo, J.R. Whinnery and Th. van Duzer, *Fields and Waves in Communication Electronics* (John Wiley & Sons, New York, 1984).
- [4] D.M. Pozar, *Microwave Engineering* (Addison-Wesley, Reading, MA, 1993).
- [5] CERN Accelerator School, RF engineering for particle accelerators, Oxford, UK, 1991, CERN 92-03, Vol. I, 1992.
- [6] L.C. Maier and J.C. Slater, *J. Appl. Phys.* **23** (1952) 68.

- [7] H. Hahn and H.J. Halama, *IEEE Trans. Microwave Theory Tech.* **MTT-16** (1968) 20.
- [8] E.L. Ginzton, *Microwave Measurements* (McGraw-Hill, New York, 1957).
- [9] E. Karantzoulis, An overview on impedances and impedance measuring methods for accelerators. Internal report ST/M-91/1, Sincrotrone Trieste, 1991.